Spatially Explicit Modeling of Hydrodynamics and Constituent Transport within the A.R.M. Loxahatchee National Wildlife Refuge, Northern Everglades, Florida

Chunfang Chen
Ehab Meselhe
Michael Waldon
Alonso Griborio
Hongqing Wang
Matthew C. Harwell

Prepared for the US Fish and Wildlife Service,
Department of Interior

by
Institute of Coastal Ecology and Engineering
University of Louisiana-Lafayette

Report #LOXA10-003
September 2010

TABLE OF CONTENTS

LIST OF FIGURES

LIST OF TABLES

Acknowledgements: The work reported here has benefitted from the technical advice of members of our project technical advisory panel, Drs. Vincent Neary (Chair), Malcolm Spaulding, and John A. McCorquodale. Advice and comments from Drs. Robert Kadlec and William Walker are also gratefully acknowledged. Funding of this study was provided, in part, by the U.S. Fish and Wildlife Service.

Disclaimer: The findings and conclusions in this article are those of the authors and do not necessarily represent the views of the U.S. Fish and Wildlife Service.

Abstract

The Arthur R. Marshall Loxahatchee National Wildlife Refuge (Refuge) is a 58,725 ha remnant of the Northern Everglades. Changes in water quantity, timing and quality have negatively impacted the Refuge. Therefore, a priority for the Refuge is to develop water quantity and quality models to identify appropriate water management strategies that will minimize negative impacts and protect fish and wildlife, while meeting flood control and water supply uses. Modeling identifies data gaps, improves understanding of impacts, and quantifies comparisons of management alternatives.

This report focuses on the development and application of a spatially explicit hydrodynamic and constituent transport surface water model for the Refuge. The spatially explicit MIKE FLOOD and ECO Lab (DHI) modeling frameworks were used to simulate the hydrodynamics and chloride (CL) transport within the Refuge. This MIKE FLOOD model dynamically links a one-dimensional model of the 100km perimeter canal with a 400m uniform grid of over 3600 two-dimensional marsh model cells, and allows for exchange of water and constituents between the two systems. Constituent transport is driven by modeled water flows and dispersion, as constituent concentrations are transformed through reactive and settling processes modeled within the ECO Lab framework. The model was calibrated for a 5-year period (2000-2004), and validated for a 2-year period (2005-2006). The graphical and statistical comparisons of stage, water depth, discharge and concentration demonstrate the applicability of this model for temporal and spatial prediction of water levels, discharge and water quality concentrations, and also demonstrate that MIKE FLOOD is a feasible alternative for modeling large wetlands that are flooded by overbank flow. The model quantifies the importance of mechanisms across the Refuge linking wetland concentration to inflow concentration and volume. Two example model applications presented here illustrate the model's ability to provide quantitative information for decision support.

1. Introduction

The Arthur R. Marshall Loxahatchee National Wildlife Refuge (Refuge) overlays Water Conservation Area 1 (WCA-1), and is managed by the United States Fish and Wildlife Service (USFWS). WCA-1 is a 58,725 ha remnant of the Northern Everglades in Palm Beach County, Florida (USFWS, 2000). Wetland loss and degradation has taken place in the Everglades, with much of this deleterious impact associated with hydrological changes (Thompson et al., 2004). The U.S. Fish and Wildlife Service (USFWS) recognized that there have been changes to the Refuge's water quantity, timing, and quality which have caused negative impacts to the Refuge's ecosystem. The Refuge is impacted by changes in water flow and stage (Brandt et al., 2000; USFWS, 2000; Brandt, 2006), excessive nutrient loading (Newman et al., 1997; USFWS, 2000), and altered dissolved mineral concentrations including chloride (Swift, 1981; Swift, 1984; Swift and Nicholas, 1987; Browder et al., 1991; Browder et al., 1994; McCormick and Crawford, 2006). According to the USFWS (2000), changes in hydroperiod and water depth patterns affect wading bird feeding patterns, apple snail reproductive output, bird and alligator nesting, and also alter the distribution of aquatic vegetation and tree islands. In addition, high concentration of nutrients in runoff causes proliferation of cattails, and other undesirable species that negatively affect the ecosystem's balance (USFWS, 2000). It is important to manage water for the benefit of fish and wildlife in the Refuge. Refuge objectives are to minimize nutrient impacts, while meeting ecosystem, flood protection, and water supply needs.

The ability to predict the effects of manipulation of water operations upon wetlands is central to the success of wetland management and restoration (Gilvear and Bradley, 2000; Hollis and Thompson, 1998). Hydrodynamic and water quality models provide the predictive tool needed for management and scientific support. A calibrated hydrodynamic and water quality model provides such information as movement of water, fate and transport of constituents, and water quality management (Kadlec and Hammer, 1988; Tsanis et al., 1998; Koskiaho, 2003). Models form the basis of information for questions regarding the hydrologic, hydrodynamic, and water quality conditions occurring under present conditions and management rules, and project how these processes would be altered by different structural changes and management scenarios.

The complexity and spatial resolution required of a model are dependent on the specific hydrological and ecological system under study, and the nature of the questions being addressed. Two types of models have been used in hydrological modeling, namely the compartment-based model (or box model), and the distributed model. The compartment-based model, which conceptualizes the system as spatially averaged compartments, has been widely used in assessing the environmental fate of chemicals (e.g., Mackay et al., 1992). It has also been applied to the Refuge modeling (Arceneaux et al., 2007; Wang et al., 2008; Wang et al., 2009; Roth et al., 2009). The most attractive feature of these models is their simplicity. The models are capable of quickly examining a broad range of alternative scenarios, which is a distinctive advantage for decision makers. However, such models are often inappropriate for site-specific applications or where detailed spatial visualization is needed. Therefore, efforts reported here have been directed towards development of distributed physically based models (Martin and Reddy, 1991; Alvord and Kadlec, 1996).

In modeling the hydrodynamics and water quality of the Refuge, a spatially explicit model was developed based on MIKE FLOOD (DHI, 2008) to provide a detailed quantitative framework to address the management tasks. This report focuses on the model development, calibration, validation, and its application to two management scenarios.

2. Study Area

2.1 Site description

The Refuge is located seven miles west of the city of Boynton Beach, Florida in the southeastern United States. It is enclosed within a levee system and a borrow canal along the interior of the levee (Richardson et al., 1990). Land use in areas bordering the Refuge varies from drained agricultural land (the Everglades Agricultural Area) on the northwest boundary, urban development to the east, and Everglades wetlands (WCA-2A) located southwest of the Refuge (Figure 1). The Refuge landscape consists of a complex mosaic of wetland communities that grade from wetter areas such as sloughs and wet prairies to sawgrass, brush, and finally tree islands occurring at the dryer end of the scale (USFWS, 2000). Refuge water conditions are controlled by the inflows and outflows through pumps and gates, rainfall, evapotranspiration (ET), and seepage.

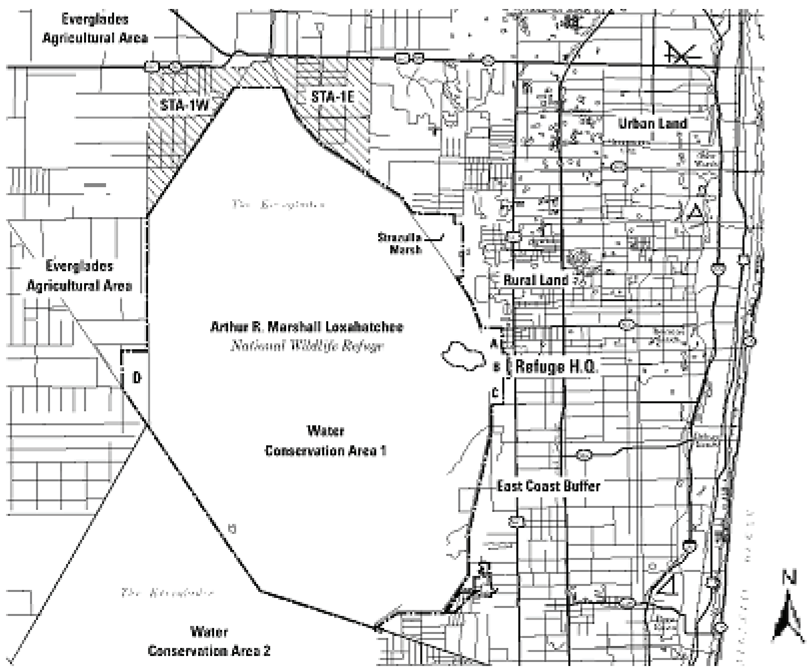

Figure 1. Boundaries of the Loxahatchee Refuge. Adapted from USFWS (2000).

Refuge topography is characterized by a fairly flat interior marsh elevation and a varying-section rim canal. The marsh elevation data were available from the United State Geological Survey (USGS) on a 400 by 400 meter grid (Desmond, 2003). The elevation ranges from 5.64 to 3.23 m (NGVD29) decreasing slightly from north to south, which at times, may direct a slow southward surface water flow (Meselhe et al., 2005) (Figure 2). It is recognized that although the modeling grid applied here was based on the best available Refuge topographic data, smaller scale topographic (microtopographic) features were not included that likely have significant influence on site-specific water depth, flow, and constituent concentrations. The perimeter canal cross-section elevation data were collected by the University of Florida's Institute of Food and Agricultural Sciences with approximate 1600 meter (~ 1 mile) resolution (Daroub et al., 2002). Figure 3 shows the Thalweg profiles for the sediment surface elevation and channel bottom elevation for the eastern canal (L-40) and the western canals (L-7 and L-39)

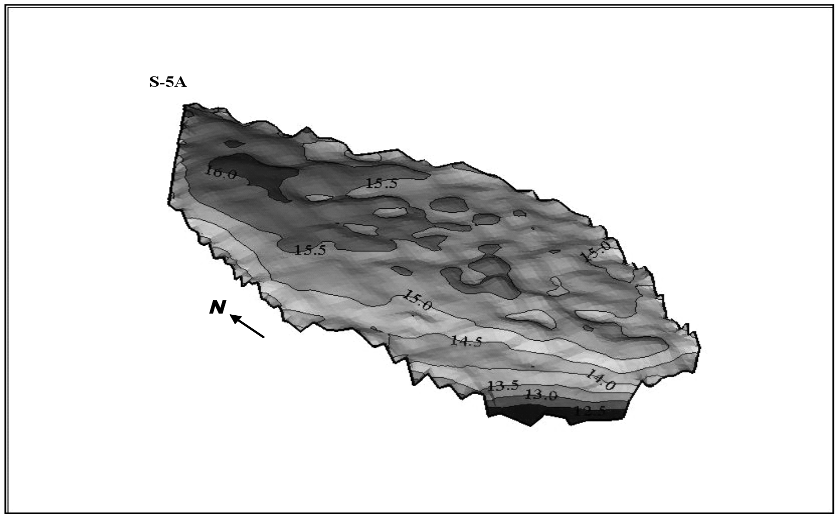

Figure 2. Topography of the Refuge (in feet NGVD 1929) based on USGS published elevations. The site of the S-5A pump station is shown in this figure. Desmond (2003)

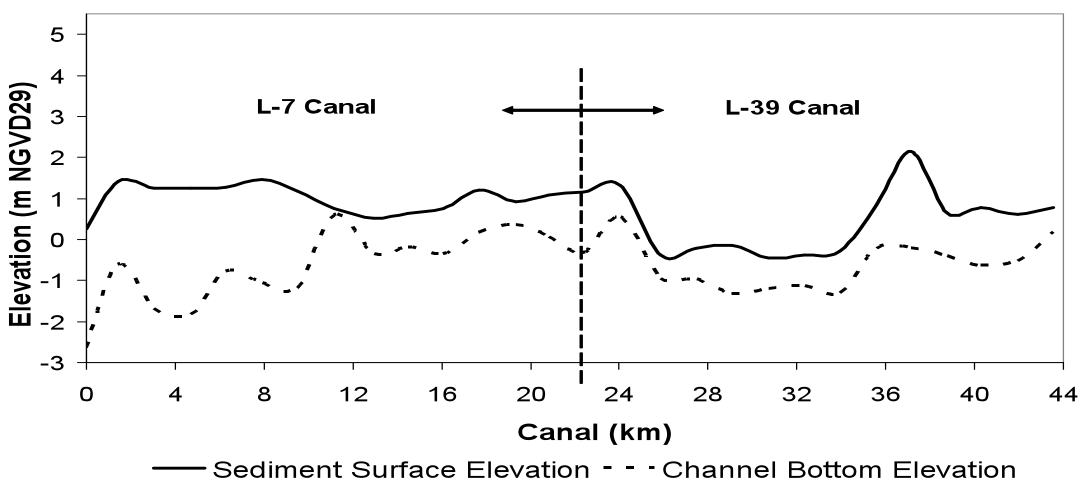

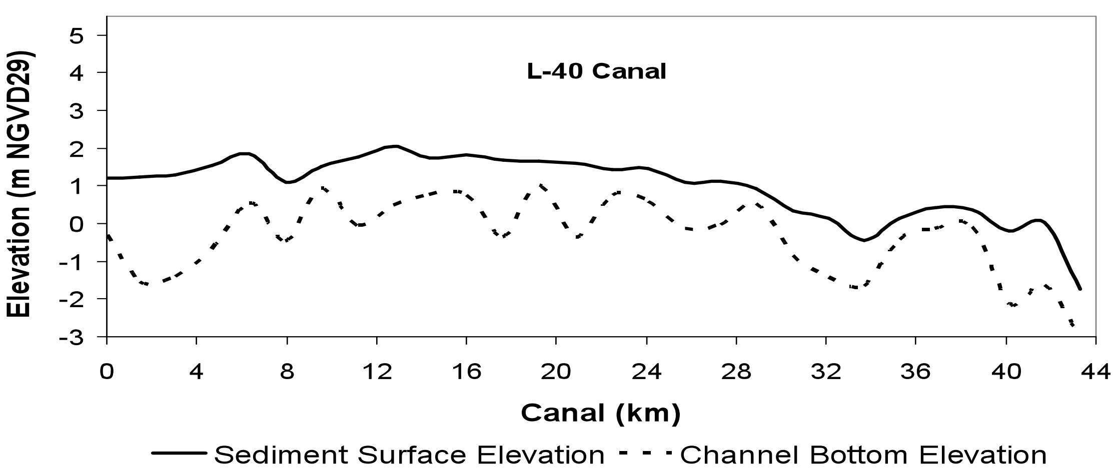

Figure 3. Thalweg profiles for the sediment surface elevation and channel bottom elevation for the eastern canal (L-40) and the western canals (L-7 and L-39) (Meselhe et al., 2005).

The primary external water sources and drains are the 19 hydraulic structures located around the perimeter canal (Figure 4). Water is pumped from the inflow pump stations S-6, S-5A, G-310, G-251, S-362, ACME-1, and ACME-2 (via gate G-94D) into the Refuge. Some of the water moves through the canals around the perimeter and is released through the southwestern and eastern gated structures of S-10E, S-10D, S-10C, S-10A, S-39, G-94C, G-94A, and G-94B. Several structures, including S-5AS, G-338, G-301, and G-300, are bidirectional. Historical flow records for these structures are maintained by the South Florida Water Management District (SFWMD) in a publicly-available online database, DBHYDRO (http://www.sfwmd.gov).

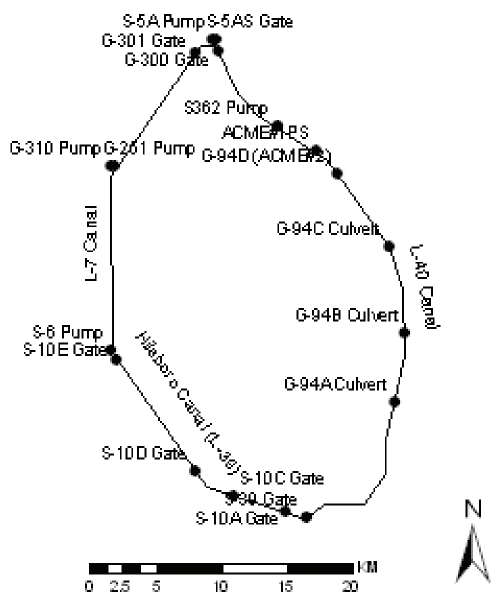

Figure 4. Location of hydraulic structures located in the Refuge

2.2 Regulation Schedule

Water levels in the Refuge are managed to meet stage regulation requirements (regulatory releases) for water supply and flood protection. Regulatory releases are mandated when the Refuge stage is in a seasonally defined flood control zone defined in a Refuge Water Regulation Schedule (WRS) and is administered by the U.S. Army Corps of Engineers (USACE, 1994), Jacksonville District. The Refuge WRS is grouped into four zones (Figure 5):

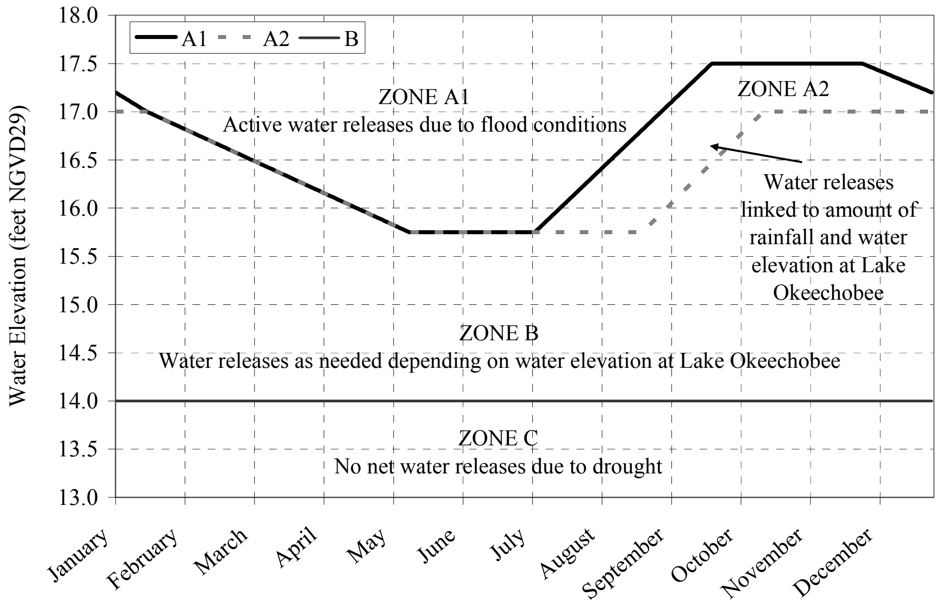

Figure 5. Water Regulation Schedule for WCA 1. Adapted from USFWS (2000).

- Zone A1 is the flood control zone from January through June. When water levels reach this zone, active water releases will be made through the S-10 spillways (and S-39 or other structure when agreed between USACE and the SFWMD).
- Zone A2 is the flood control zone from July through December. In this zone water levels in the Refuge are permitted to reach a maximum of 5.334 m (17.5 ft) NGVD 29. Excess water is released, typically from the S-10 and S-39 spillways, based on USACE forecasts. If Lake Okeechobee's stage is above the Refuge's stage or no more than one foot below, then water supply releases from the Refuge must be preceded by an equivalent volume of inflow.
- Zone B is the water supply zone. Water levels range from a minimum of 4.267 m (14.0 ft) NGVD 29 up to a maximum of 5.334 m (17.5 ft) NGVD 29. When water levels in the Refuge are within this zone, water releases are allowed, as needed depending on the water level at Lake Okeechobee. If Lake Okeechobee's stage is above the Refuge's stage or no more than one foot below, then water supply releases from the Refuge must be preceded by an equivalent volume of inflow. This is the zone considered to be most beneficial to fish and wildlife of the Refuge (USFWS, 2000).
- Zone C is the lowest zone where water levels drop to 4.267 m (14 ft) NGVD 29 or lower. If water supply releases do occur, they must be preceded by an equivalent volume of inflow; because water levels in the Refuge interior are very low, significant attention is paid to the effects on the ecosystem when water management decisions are made in this zone.

2.3. Field Data

The daily-averaged structural inflow and discrete concentrations measured using irregularly scheduled grab samples were obtained from DBHYDRO. Daily data of precipitation and evapotranspiration were collected from available gages (Meselhe et al., 2005) (Figure 6). Five continuous water level stations maintained by USGS are located in the marsh, and another water level station (1-8C) is located in the eastern (L-40) canal (Figure 6). Additionally, water depth, termed Depth to Consolidated Substrate (DCS), was measured by the U.S. Fish and Wildlife Service (USFWS, 2007) when marsh water quality samples were collected at 39 canal and marsh stations (enhanced stations, Figure 7) for monthly grab samples.

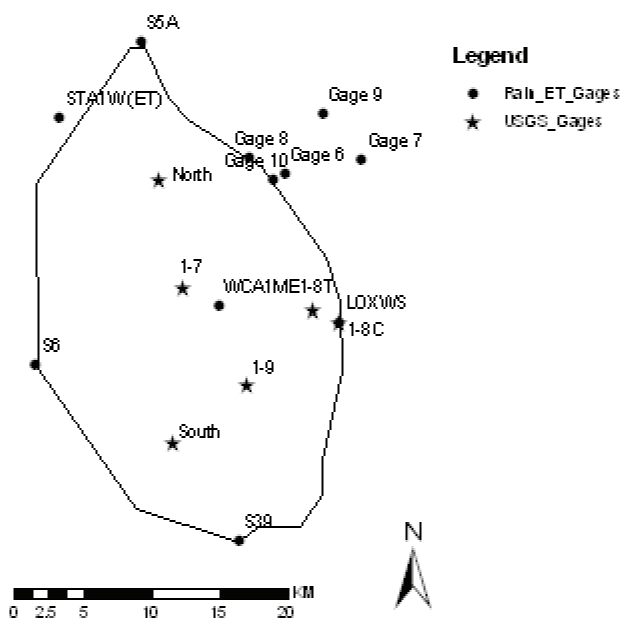

Figure 6. Location of rain gages, ET site, and water level stations in the Refuge

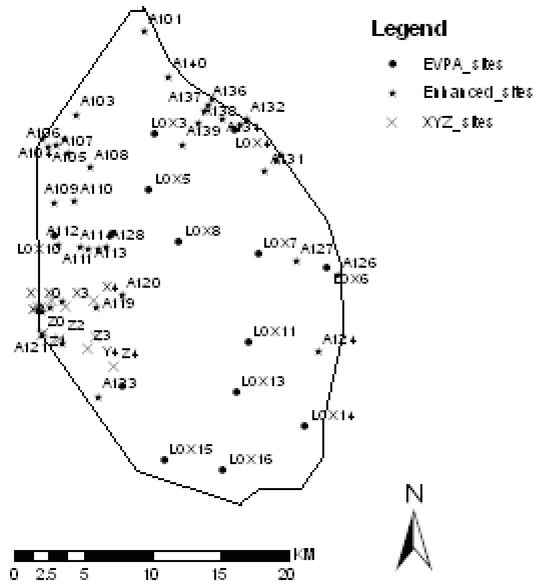

Figure 7. Water quality monitoring sites located in the Refuge. (Enhanced sites, labeled LOXA elsewhere, are labeled A here for brevity)

Chloride concentration was collected from five data sources: 1) EVPA water quality stations; 2) enhanced water quality monitoring stations; 3) district transect monitoring sites (also known as the XYZ sites); 4) water quality monitoring sites located at the structures; and 5) additional independent monitoring sites (Meselhe et al., 2005) (Figure 7).

3. Methods

3.1 MIKE FLOOD

MIKE FLOOD is a spatially distributed and physically based modeling environment. It integrates a 1-D channel model (MIKE 11) with a 2-D surface flow model (MIKE 21) into a single, dynamically coupled system through user-defined links.

3.2 Hydrodynamic Model

The hydrodynamic model in MIKE 21 solves the unsteady depth-integrated 2-D continuity and momentum equations. The hydrodynamic model in MIKE 11 solves the fully dynamic Saint Venant equations. MIKE 11 also simulates a broad range of hydraulic structures including weir, gate, bridge, culvert, and control structure. Among those, control structure is employed in this model to simulate regulatory releases.

3.3 Advection-Dispersion (AD) Model

The AD models in MIKE 21 and MIKE 11 solve the advection-dispersion equation. The mass balance relationship of the marsh including the reactive and settling processes for water constituent is defined in the open-source ECO Lab module. Chloride is simulated as a conservative tracer in the AD models.

4. Model Setup

4.1 MIKE 21

The MIKE 21 model domain is represented by a uniform Cartesian grid of 400 m resolution based on the USGS survey (Desmond, 2003). Spatial map was generated for rainfall using inverse-distance method based on measurements at available stations. For ET, when water depth was low, the measured ET was reduced using a reduction factor (Arceneaux et al., 2007):

$$ET_{act} = f_{ET} * ET_{obs} \tag{3}$$

$$f_{ET} = \max(f_{ET\min}, \min(1, \frac{H}{H_{ET}})) \tag{4}$$

where

$f_{ET\min}$ minimum reduction of ET due to shallow water depth (%)
H estimated water depth (m)
H_{ET} depth above which ET is not reduced (m)

Here, $f_{ET\min}$ and H_{ET} are determined through calibration. The spatial map of ET was generated by first interpolating the observed water level using inverse-distance method and transformed to a spatially varied water depth. The water depth was then substituted into Eq. 4 to calculate actual ET. As groundwater is not included in MIKE 21, seepage was modeled through ET. It was assumed to be constant and evenly distributed across the marsh. Resistance of the marsh was estimated based on vegetation (Richardson et al., 1990) from 1987 imagery. The vegetation was classified into six categories used by the SFWMD (2000), which was obtained from the vegetation mapping of Richardson et al. (1990): sawgrass, cattail, open water and sloughs, wet prairie, tree island, and brush. The conveyance was derived in GIS based on this classification, and was expressed in Manning's M ($m^{1/3}/s$), the reciprocal of Manning's n (Table 1).

Table 1. Manning's n for different vegetation classes

Vegetation type	Manning's n ($s/m^{1/3}$)
sawgrass	4
cattail	4
open water and sloughs	0.8
wet prairie	4
tree island	2
brush	2

The velocity based Smagorinsky formula (DHI Water & Environment, 2008d) was selected for turbulence with the Smagorinsky constant set to 0.5. The two options provided for dispersion – independent of velocity and proportional to velocity were tested. For the current-independent option, concentrically distributed dispersion coefficients in six levels were defined, gradually increasing from the peripheral zones towards the interior. Constant wet and dry depositions were assumed for chloride. The initial water level was estimated by averaging the observations at 1-7, 1-8T, and 1-9. The spatially varied initial concentration was generated based on the observed data at interior stations. A 5-min time step was used when simulating hydrodynamics only. To maintain stability for the AD module, the time step was reduced to 3-min when simulating chloride.

4.2 MIKE 11

The MIKE 11 channel network was defined using canal cross-section data collected. The historical daily average inflows and discrete chloride concentrations stated in the previous section were imposed at the inflow boundaries. Control structures were applied at the four regulatory outflow structures (S-10A, S-10C, S-10D, and S-39), for which the discharge was a function of the difference in stage between station 1-8C and the WRS zone A1 floor (Figure 5). The discharge - stage difference relationship for the S-10 structures (S-10A, S-10C and S-10D) was derived based on the observed data of 1/1/1995-8/31/2007 (Figure 8). The discharge of S-39 was estimated using the ratio of the historical regulatory release of S-39 to the S-10 structures. Water supply discharge at S-39 was estimated using historical daily average supply discharge. For the non-regulatory outflow structures, historical discharge data were imposed at the boundaries.

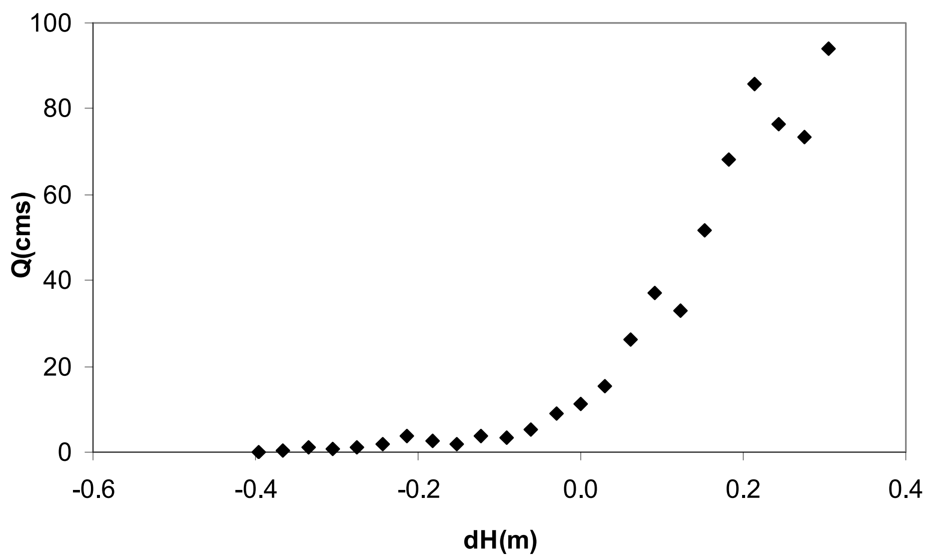

Figure 8. Discharge and stage difference relation based on historic data of S10 outflows (1/1/1995-8/31/2007).

Uniform Manning's n was assumed for resistance and was to be calibrated. Dispersion was modeled using the exponential function

$$D = aV^b \tag{5}$$

where V is the velocity, *a* and *b* were calibration parameters. Spatially uniform (while temporally variable) precipitation and evaporation were assumed. As groundwater is not included in MIKE 11, seepage was assumed to be constant and modeled as uniformly distributed outflow through the boundary. It was determined through calibration. The same wet and dry depositions as used for the marsh were also applied for the canal. The stage observed at 1-8C was used for the initial canal stage estimation. The average of the observed concentration at canal stations was used for the initial canal concentration. The same time step used in MIKE 21 was applied.

4.3 Coupled Model

Initially, the MIKE 11 channels were linked with the cells of MIKE 21 through the lateral link provided by MIKE FLOOD. Tests revealed that this option works well for the hydrodynamics, but introduces significant mass error for the AD module. To resolve this problem, the standard link was used.

5. Calibration and Validation

A 5-year period (2000-2004) was selected for model calibration. This period contains both high and low flow years, and is helpful to evaluate the model's capability to capture the variation of hydro-pattern. The 2-year period of 2005-2006 was selected for model validation. The model was first calibrated for stage, and then for chloride concentration. The fine tuning of parameters was restricted to the physically realistic range. Statistical measures were calculated to quantify the model performance.

The parameters involved for hydrodynamic calibration include roughness and seepage for the marsh and the canal, dry and wet depths for the marsh, ET reduction factor, and minimum depth for ET reduction. Preliminary results showed that stage was not sensitive to roughness in general, and was particularly insensitive to canal roughness. The calibrated canal Manning's n was 0.03 $s/m^{1/3}$. The stage was found to be sensitive to the overall seepage in the system, regardless of the ratio between the marsh and the canal. The total seepage was calibrated to be 4.5 m^3/s. Dry and wet depths account for the drying and rewetting processes of the marsh cells. A number of values were tested for dry depth ranging from 0.01 m to 0.05 m. Wet depth was examined over the range from 0.012 m to 0.1 m. These depth parameters had insignificant influence to predicted stage. For ET reduction factor and the minimum depth for ET reduction (Eqs. 3 and 4), a larger ET reduction factor or higher minimum depth reduce actual ET, and result in increased water level. Several sets were calibrated for these two parameters to envelop the physical limits for each. Calibration results varying these ET parameters indicated that different combinations give similar predictions; thus, this parameter set is not uniquely defined through stage calibration.

The calibration parameters for chloride include aerial (wet and dry) depositions, seepage, and dispersion in the marsh and the canal, and transpiration in the marsh. The wet and dry

depositions calibrated from a companion study (Arceneaux et al., 2007) provided reasonable results, and were adopted in this model. Transpiration was defined using a single constant fraction of ET (Zhang et al., 2002; Andersen et al., 2001; Arceneaux et al., 2007).
Chloride concentration was found to be highly sensitive to transpiration. The calibrated transpiration fraction of ET was 35%. For dispersion in the marsh, the velocity-independent option provided better predictions compared to the velocity-dependent option, and was adopted for this model. The six calibrated dispersion coefficients were 0.001, 0.3, 0.5, 0.8, 1.5, and 2.0 m^2/s increasing from the fringe marsh to the most interior marsh. These values fall within the range given by Kadlec and Knight (1996). In calibrating the dispersion coefficients, numerical dispersion was considered, especially for the fringe marsh, which led to the relatively large gradient between the two outer most levels. For the canal dispersion, a uniform and constant coefficient was applied (i.e., b=0 in Eq. 5). Chloride transport in the canal is dominated by advection, and chloride concentration shows only slight variation to change in canal the dispersion coefficient. The final calibrated canal dispersion was 50 m^2/s, which is not atypical for natural channels (Bowie et al., 1985).

Several hydrodynamic model parameters were found to have only minor impacts on predicted stage, but had significant impact on computed chloride concentration. This difference in parametric sensitivity supported a more reliable hydrodynamic model calibration for several parameters including dry and wet depths, the seepage ratio between the marsh and the canal, and marsh roughness. The dry and wet depths were identified through chloride calibration to be 0.05 and 0.052 m, respectively. The chloride overall mass balance is sensitive to the ratio of seepage through the marsh and the canal because the typical canal concentration is much higher than that of the marsh, and the canal seepage transports more chloride mass per unit of flow than the marsh seepage. The final calibrated ratio of marsh and canal seepage volumes is 1:1. Early stage calibration attempts over-predicted chloride concentration in the western marsh near the S-6 pump station (Figure 4). We conjecture that this anomaly is caused by failure of the 1987 imagery (Richardson et al., 1990) to capture recent vegetation change in this area. Vegetation in this area was re-evaluated by inspecting the images from Google Earth (http://earth.google.com). An enlargement of a strip of dense vegetation along the perimeter canal in the southwestern Refuge was observed, examined and found to be consistent with anecdotal field observations of dense cattails invading areas surrounding water quality sampling sites. To account for such change in the model, vegetative resistance was increased in this area. The calibrated parameters are given in Table 2.

Table 2. Calibrated hydrodynamic and chloride model parameters

	Parameters	Unit	Value
Marsh	Roughness	$m^{1/3}/s$	0.125-0.5 (spatial variable)
	Seepage	m^3/s	2.25 (spatial variable)
	dry/wet depth	m	0.05/0.052
	depth reduction factor		0.2
	depth reduction boundary	m	0.2

	ET percent as transpiration	%	35
	dispersion	m^2/s	0.001- 2 (6 concentric zone)
Canal	roughness	$s/m^{1/3}$	0.03
	seepage	m^3/s	2.25
	dispersion	m^2/s	50
Marsh and Canal	Chloride wet deposition	mg/L	2
	Chloride dry deposition	mg/m^2-yr	500

6. Results

6.1 Stage and Depth

In general, the model showed good agreements with the observed water levels and captured the overall trends and seasonal variations, and calibration errors are of reasonable magnitude (Figure 9). Discrepancies between simulated and observed stage are largely attributed to uncertainty in model inputs, and temporal aggregation in daily averaged flows and precipitation used for the boundaries. The model is not expected to capture stage response to events of time scale smaller than daily. This is more apparent for low stage events, such as the dry period during May 2001 in the canal when small diel fluctuation in canal stage was observed. Uncertainty in ET estimation also likely contributes significantly to calibration error because only one ET station located to the northwest of the Refuge is available for the modeling period. Major deviations are observed during the exceptionally dry and low stage period in 2001 for the canal and the adjacent marsh station of 1-8T. As previously noted, this model does not simulate groundwater when observed water levels fall below the marsh surface. As no deficit from below-ground stage conditions needs to be replenished prior to rewetting, the MIKE FLOOD model does tend to recover too quickly from extreme drought. Statistics for the calibration and validation (Tables 3 and 4) show that the hydrodynamic model was calibrated well with high correlation coefficients (all above 0.85), low bias (all less than 0.1 m), and high Nash-Sutcliffe efficiency (all above 0.5 except for 1-8C for the validation period).

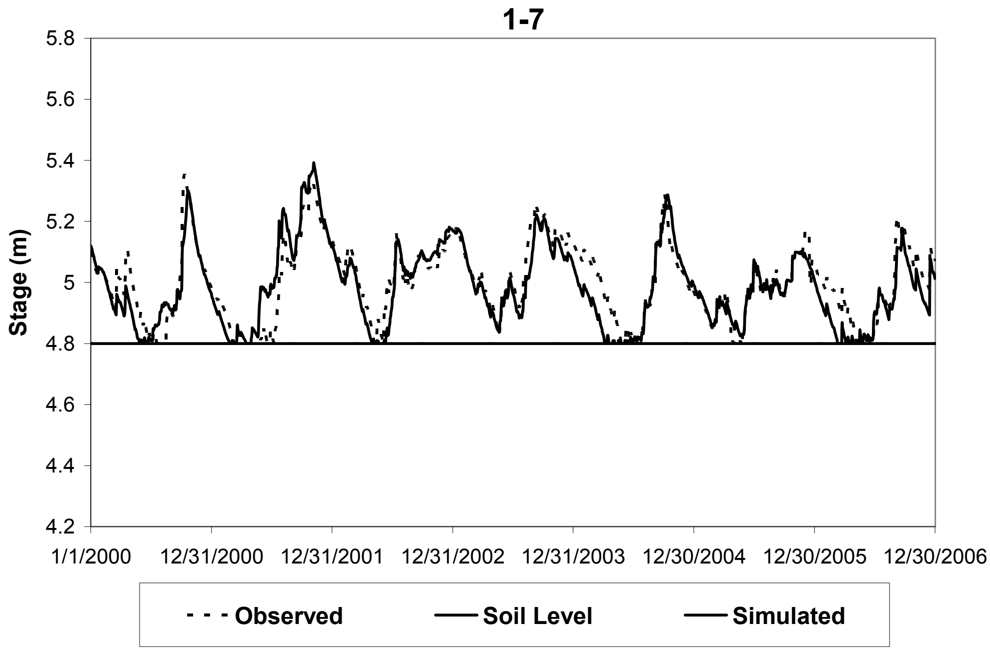
1-7
Stage (m)
5.8
5.6
5.4
5.2
5
4.8
4.6
4.4
4.2
1/1/2000
12/31/2000
12/31/2001
12/31/2002
12/31/2003
12/30/2004
12/30/2005
12/30/2006
Observed
Soil Level
Simulated

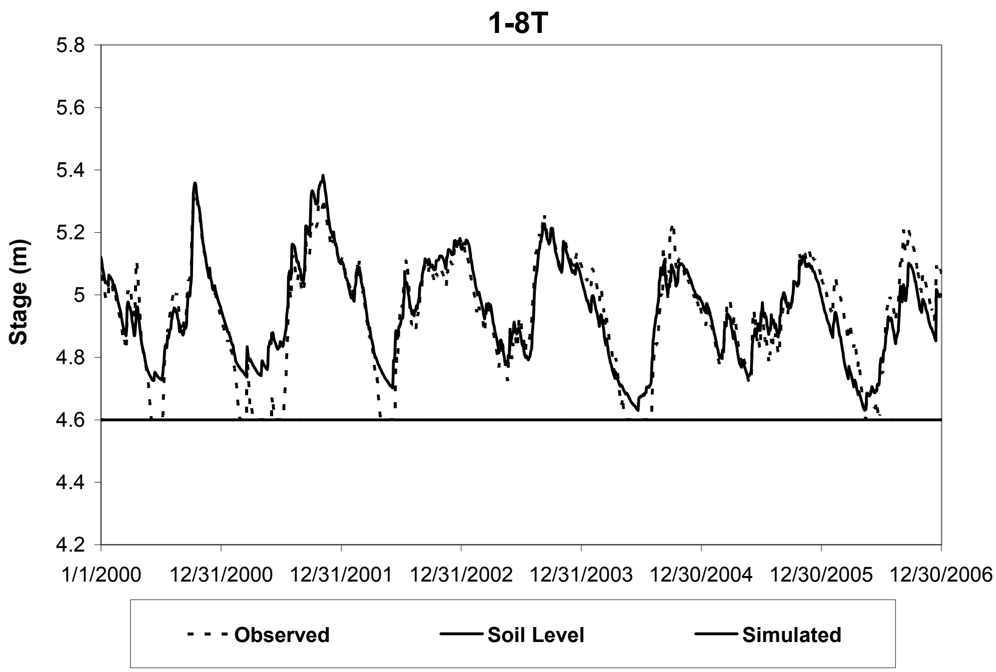
1-8T
Stage (m)
5.8
5.6
5.4
5.2
5
4.8
4.6
4.4
4.2
1/1/2000
12/31/2000
12/31/2001
12/31/2002
12/31/2003
12/30/2004
12/30/2005
12/30/2006
Observed
Soil Level
Simulated

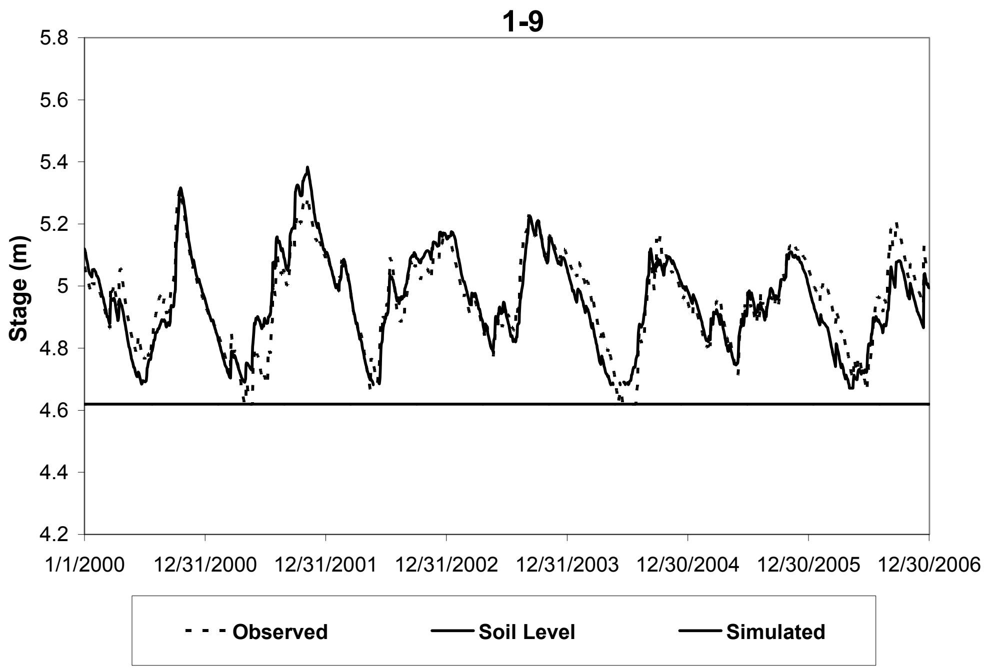
1-9
5.8
5.6
5.4
5.2
5
4.8
4.6
4.4
4.2
Stage (m)
1/1/2000
12/31/2000
12/31/2001
12/31/2002
12/31/2003
12/30/2004
12/30/2005
12/30/2006
Observed
Soil Level
Simulated

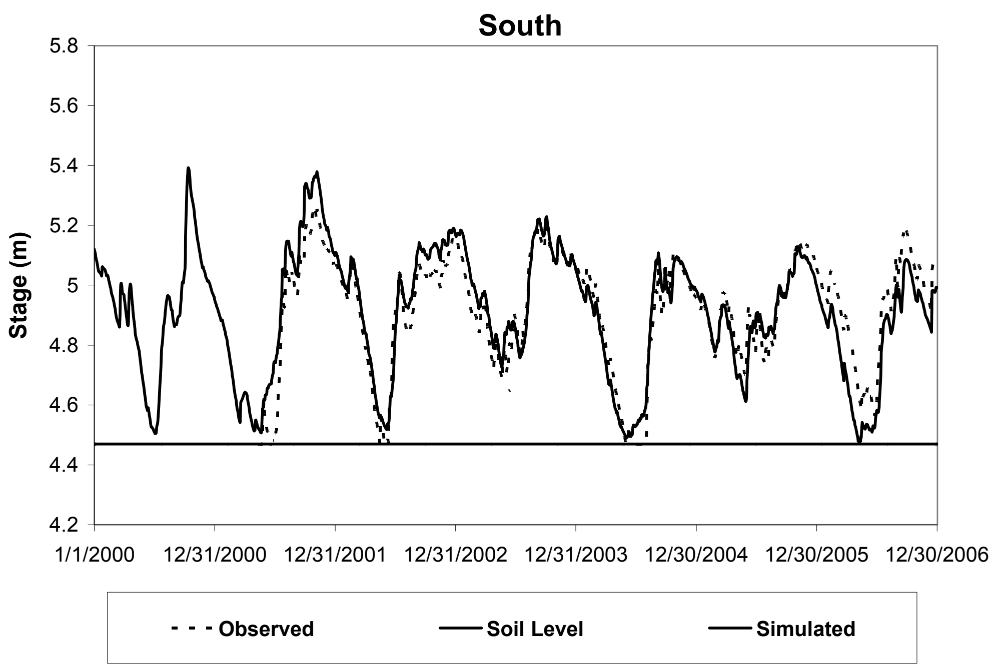
South
5.8
5.6
5.4
5.2
5
4.8
4.6
4.4
4.2
Stage (m)
1/1/2000
12/31/2000
12/31/2001
12/31/2002
12/31/2003
12/30/2004
12/30/2005
12/30/2006
Observed
Soil Level
Simulated

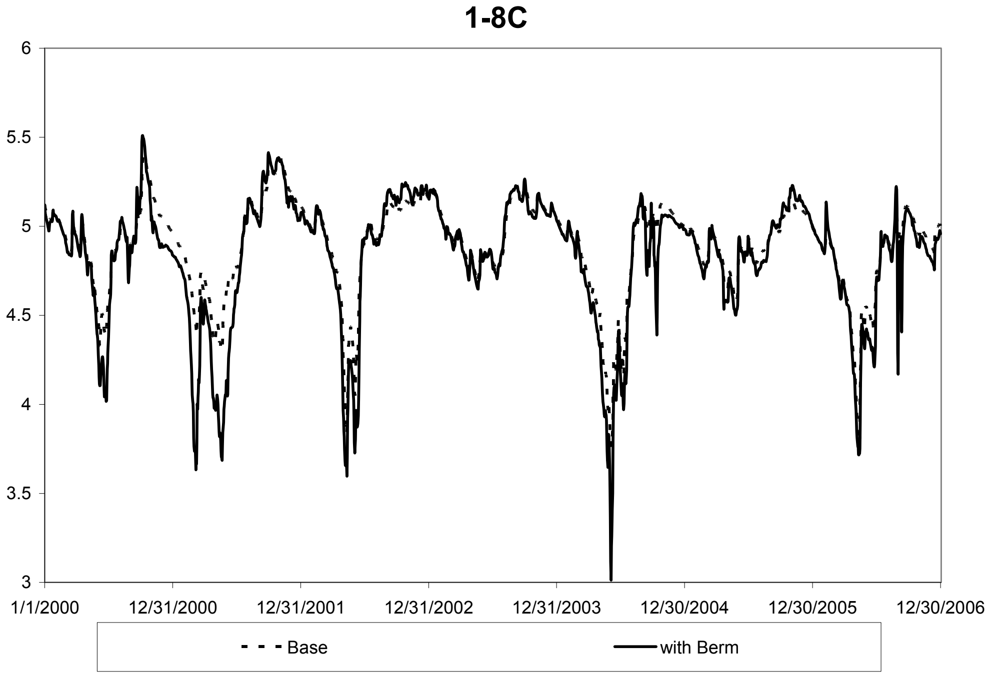

Figure 9. Comparisons of modeled and observed water level at marsh and canal stations.

Table 3. Calibration statistics of water level (2000-2004)

Station	Bias (m)	RMSE (m)	Average Observed (m)	Average Model (m)	SD Observed (m)	SD Model (m)	SD Error (m)	Variance reduction	R (Correl Coef)	r2	Nash-Sutcliffe Eff
North	-0.04	0.08	5.10	5.04	0.12	0.14	0.07	0.62	0.86	0.74	0.51
1-7	-0.01	0.07	5.01	5.00	0.13	0.14	0.06	0.77	0.89	0.80	0.77
1-8T	0.03	0.08	4.94	4.97	0.20	0.17	0.07	0.87	0.94	0.89	0.85
1-9	0.00	0.06	4.96	4.97	0.16	0.16	0.06	0.86	0.94	0.88	0.86
South	0.04	0.07	4.91	4.93	0.21	0.22	0.06	0.92	0.96	0.93	0.89
1-8C	-0.03	0.09	4.94	4.90	0.28	0.27	0.08	0.92	0.96	0.92	0.91

Table 4. Validation statistics of water level (2005-2006)

Station	Bias (m)	RMSE (m)	Average Observed (m)	Average Model (m)	SD Observed (m)	SD Model (m)	SD Error (m)	Variance reduction	R (Correl Coef)	r2	Nash-Sutcliffe Eff
North	-0.02	0.04	5.01	4.99	0.09	0.09	0.04	0.79	0.90	0.80	0.75
1-7	-0.03	0.05	4.97	4.95	0.10	0.09	0.05	0.79	0.89	0.79	0.72
1-8T	-0.03	0.07	4.94	4.90	0.14	0.12	0.06	0.80	0.89	0.80	0.74
1-9	-0.04	0.06	4.94	4.91	0.12	0.11	0.05	0.81	0.90	0.81	0.72
South	-0.06	0.09	4.92	4.86	0.15	0.16	0.07	0.81	0.91	0.84	0.66
1-8C	-0.09	0.14	4.94	4.84	0.17	0.21	0.11	0.57	0.85	0.73	0.24

Comparison of modeled surface water depth with DCS measured during monthly water quality sample collections provided an independent test over a wider spatial extent than was provided by recording stage gages in the marsh (Figure 10). Monthly water quality samples and DCS are collected in the vicinity of a fixed location. Because they are not taken at exactly the same location each month, DCS measurements are expected to have lower precision than measurements at fixed location stage gages. Furthermore, a positive bias under more shallow conditions was expected because samplers search for a sampling location in the vicinity of the marked sampling site with a minimum 10 cm clear water depth. Despite these complications, the model presented a good fit to the observed variations in DCS at most sites. This further verifies that the model can provide reliable predictions beyond the established stage gage network. It also demonstrates that the effort of carefully measuring DCS during sampling provides valuable data. Observed marsh DCS ranged from a low below 0.1 m typically occurring more in the north, to a high of 0.65 m in the south.

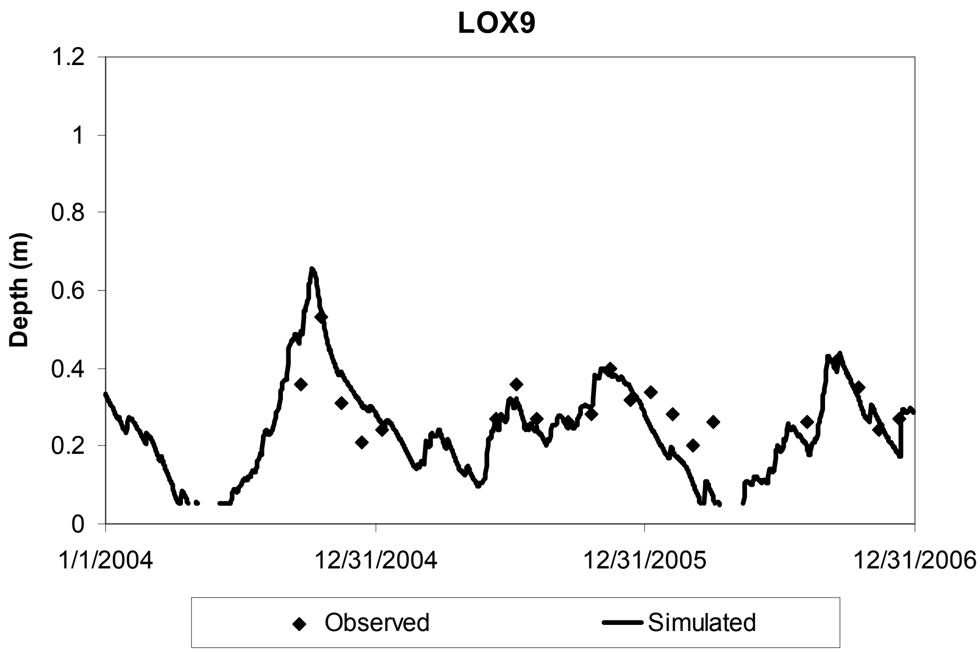

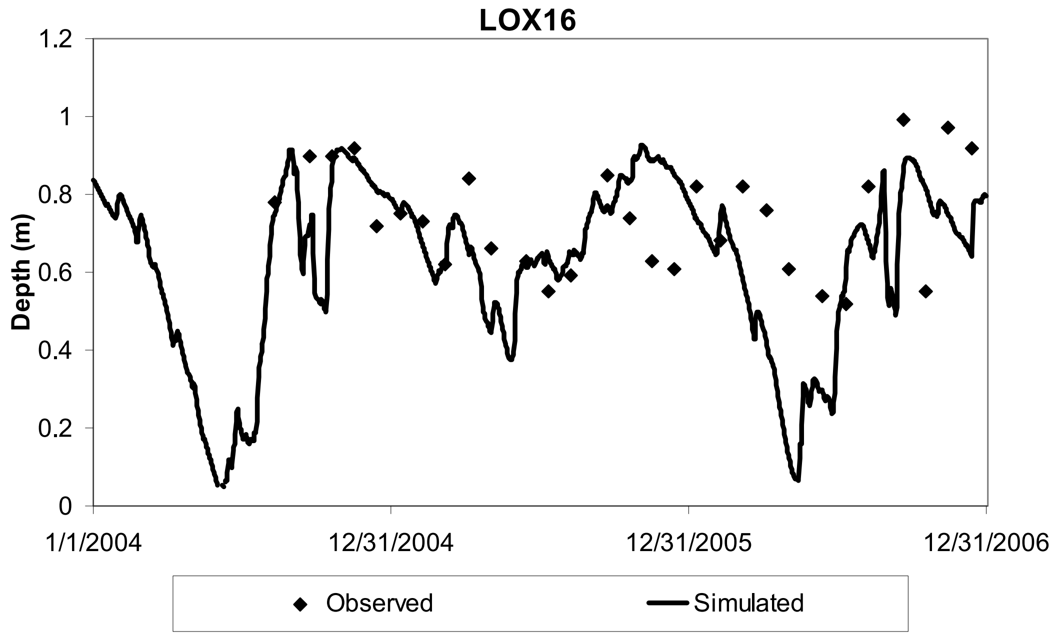
LOX16
Depth (m)
1.2
1
0.8
0.6
0.4
0.2
0
1/1/2004
12/31/2004
12/31/2005
12/31/2006
Observed
Simulated

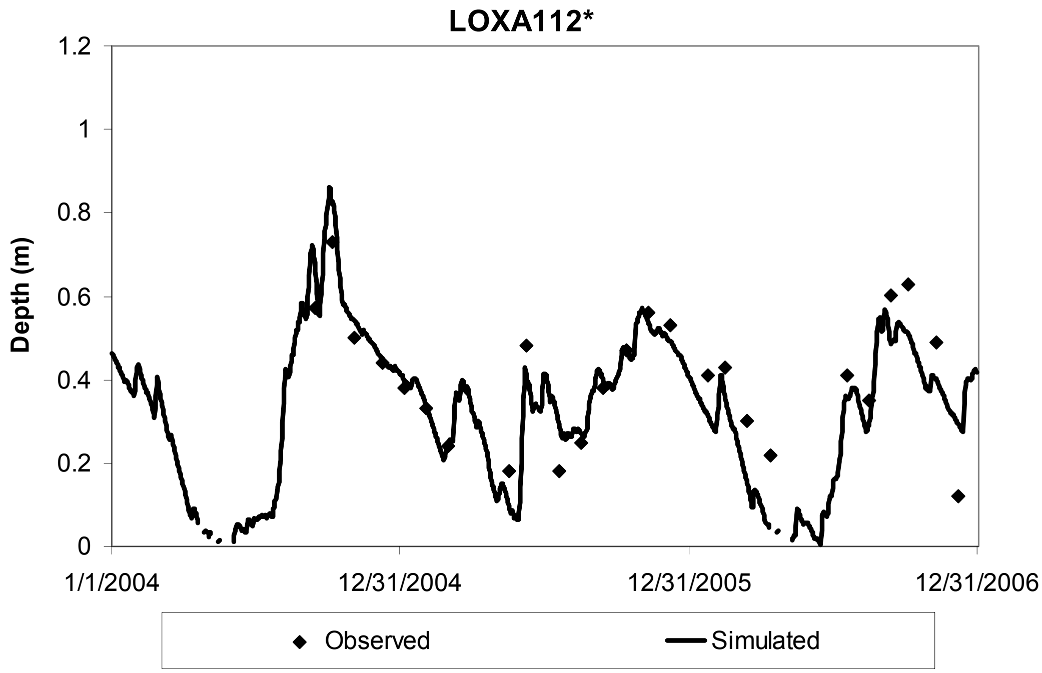
LOXA112*
Depth (m)
1.2
1
0.8
0.6
0.4
0.2
0
1/1/2004
12/31/2004
12/31/2005
12/31/2006
Observed
Simulated

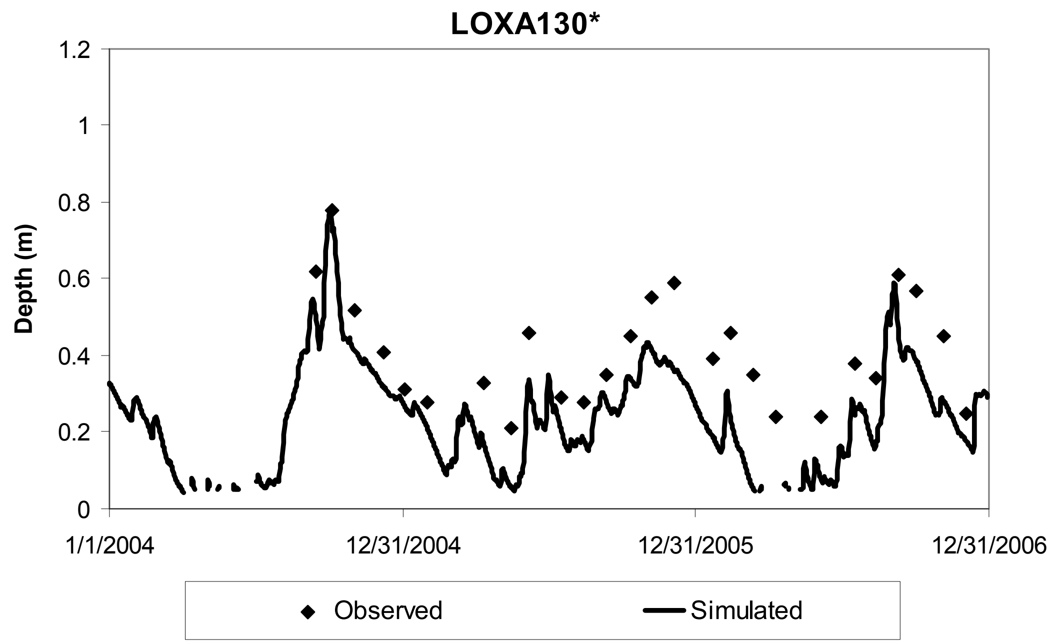

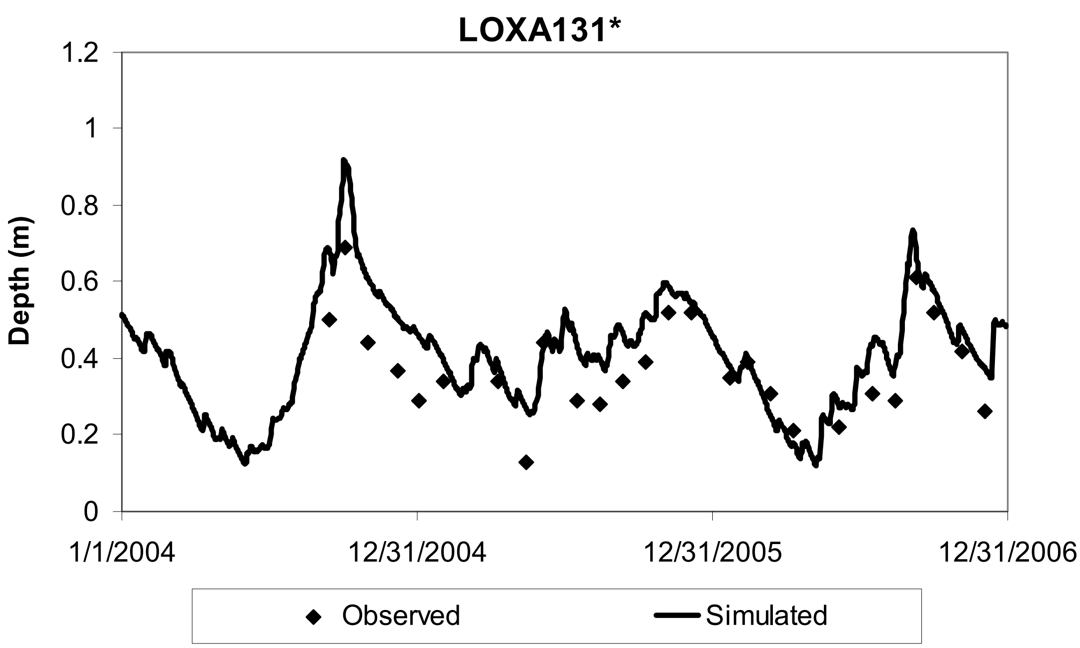

Figure 10. Comparisons of simulated and observed water depth at selected DCS stations.

*: the "LOXA" stations are labeled as "A" stations in Figure 7

The DCS data also provide an independent test of the topographic data used in model development, because at high stage when there are no large inflows or outflows the water stage is generally flat across the Refuge. Thus, stage minus DCS provides a good estimate of soil elevation at the sampling site. At the neighboring stations of LOXA130 and LOXA131, it was observed that even though the observed data displayed a similar pattern, the model predictions showed drastically different patterns. Such modeled differences are conjectured to be related to inadequacy of spatial resolution and sampling bias for characterization of topography and vegetation. The influence of local topographic and vegetation features with a scale below the 400 m model resolution may have significant influence on site-specific observations.

6.2 Discharge

The simulated discharges of the four regulatory structures (S-10A, S-10C, S-10D and S-39) were compared with the recorded data (Figure 11). The daily discharge obtained at noon was aggregated to annual discharge. Agreement between the predicted and recorded annual outflows at the four structures individually and combined is not much greater than the uncertainty associated with discharge estimation at gates and pumps (Ansar and Chen, 2009). Statistics of annual discharge over the entire period of simulation (Table 5) demonstrate that the model does predict individual structure flows well, but is more reliable in predicting overall outflow.

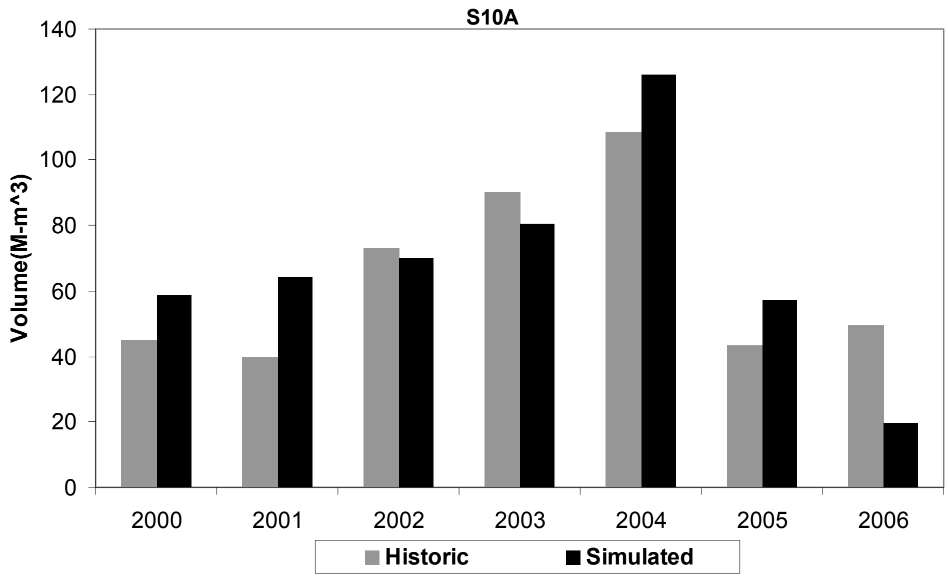

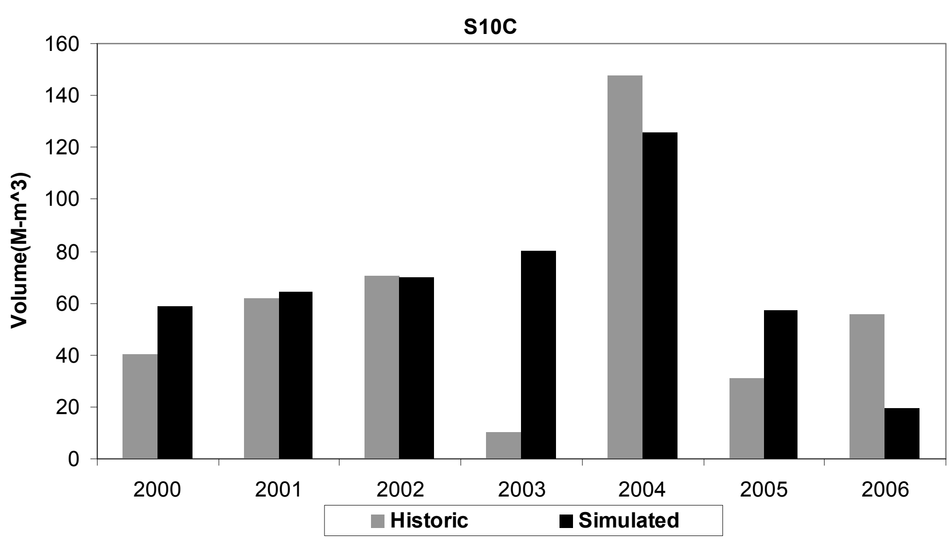

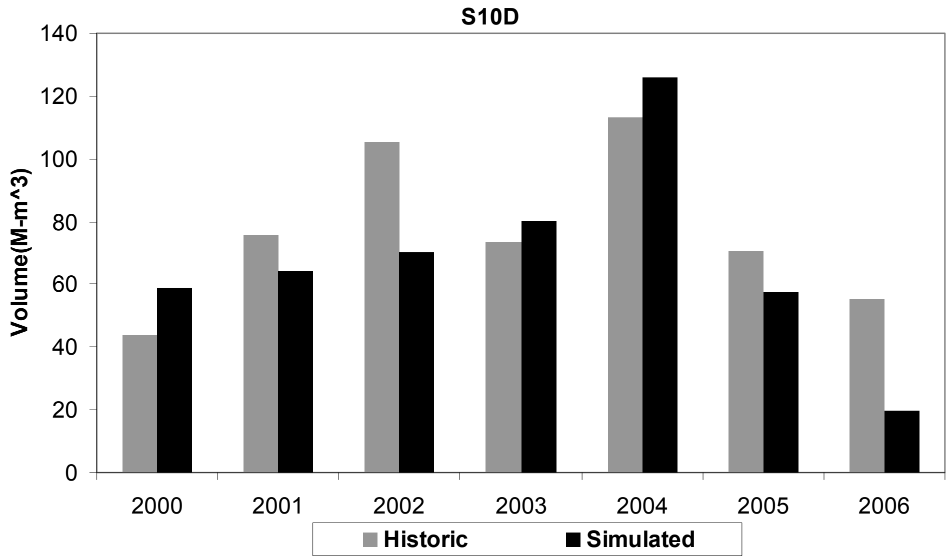
S10D
Volume(M-m^3)
0
20
40
60
80
100
120
140
2000
2001
2002
2003
2004
2005
2006
Historic
Simulated

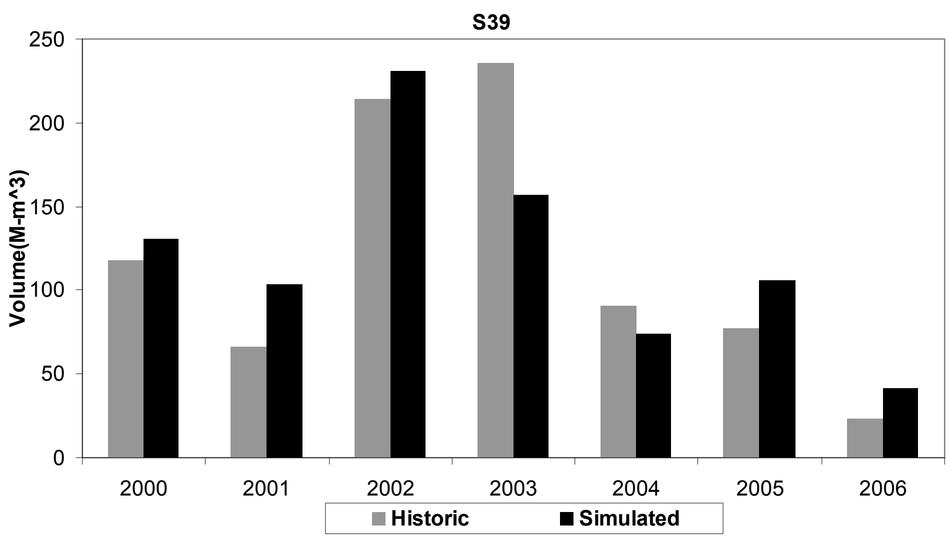
S39
Volume(M-m^3)
0
50
100
150
200
250
2000
2001
2002
2003
2004
2005
2006
Historic
Simulated

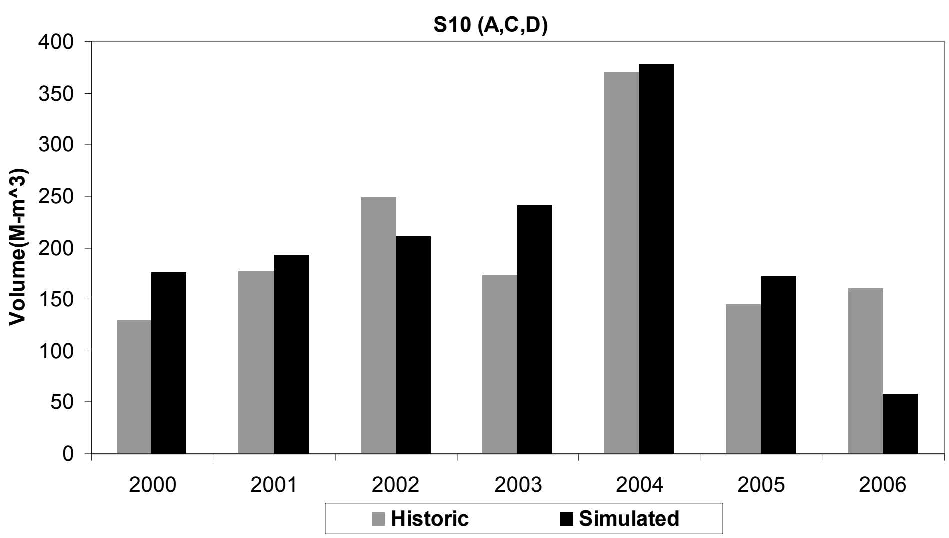
S10 (A,C,D)
Volume(M-m^3)
0
50
100
150
200
250
300
350
400
2000
2001
2002
2003
2004
2005
2006
Historic
Simulated

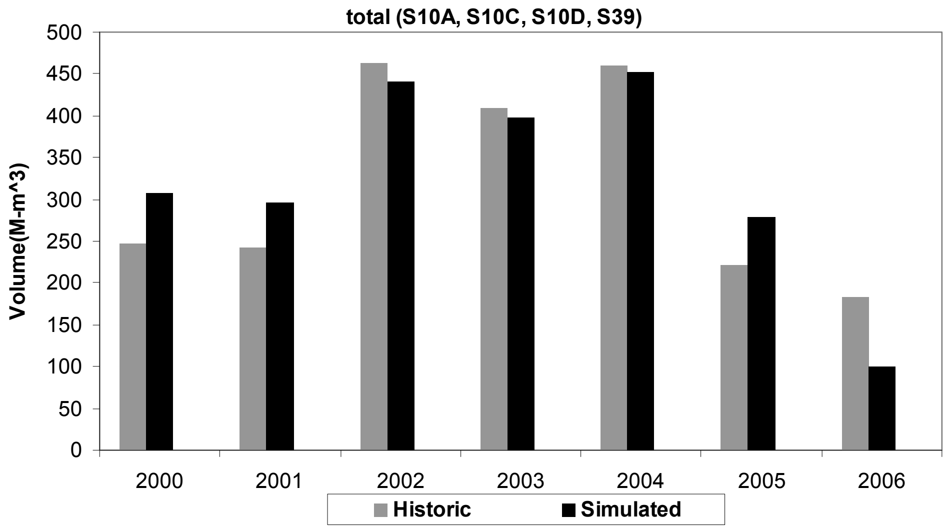

Figure 11. Comparisons of simulated and measured annual discharge at the outflow structures individual and combined.

6.3 Chloride (CL) Concentration

The modeled chloride concentration was compared with the measured data of the EVPA, XYZ, enhanced water quality network (data available after August 2004, alternatively termed LOXA or A stations), and the canal hydraulic structure samples for the calibration and validation periods. There are 54 marsh and 11 canal stations. Among those, marsh sampling was typically monthly, but sampling at canal structures was typically irregular. Several representative stations, which broadly cover the Refuge, were selected to illustrate the diversities of chloride concentration over the Refuge (Figure 12). For those selected stations, the comparison of time series, scatter plot, and accumulative exceedance percentage curve of observed and predicted chloride concentration showed seasonal patterns and instances of high chloride canal water intruding into the peripheral marsh. The occasional gaps in the model results seen in the time series graphs reflected periods where a cell was dry. Gaps in marsh sampling data reflected instances when water was too shallow to sample (i.e., depth of clear water was less than 10 cm). The corresponding statistics for those stations are given in Tables 6 and 7 for the calibration and validation periods, respectively.

Table 5. Statistics of annual discharge for the calibration and validation period (2000-2006)

Station	Bias (m^3*10^6)	RMSE (m^3*10^6)	Average Observed (m^3*10^6)	Average Model (m^3*10^6)	SD Observed (m^3*10^6)	SD Model (m^3*10^6)	SD Error (m^3*10^6)	Variance reduction	R (Correl Coef)	r2	Nash-Sutcliffe Eff
S-10A	3.91	18.11	64.18	68.09	26.92	31.85	19.1	50%	0.8	0.64	0.47
S-10C	8.38	33.25	59.71	68.09	43.83	31.85	34.76	37%	0.62	0.38	0.33
S-10D	-8.58	21.55	76.66	68.09	25.06	31.85	21.35	27%	0.74	0.55	0.14
S-39	2.7	36.96	117.75	120.45	78.67	61.31	39.81	74%	0.87	0.75	0.74
S-10ACD	3.71	53.07	200.55	204.26	83.69	95.54	57.18	53%	0.8	0.65	0.53
S-10ACD+S-39	6.41	49.96	318.3	324.71	120.72	121.74	53.51	80%	0.9	0.82	0.8

(a)

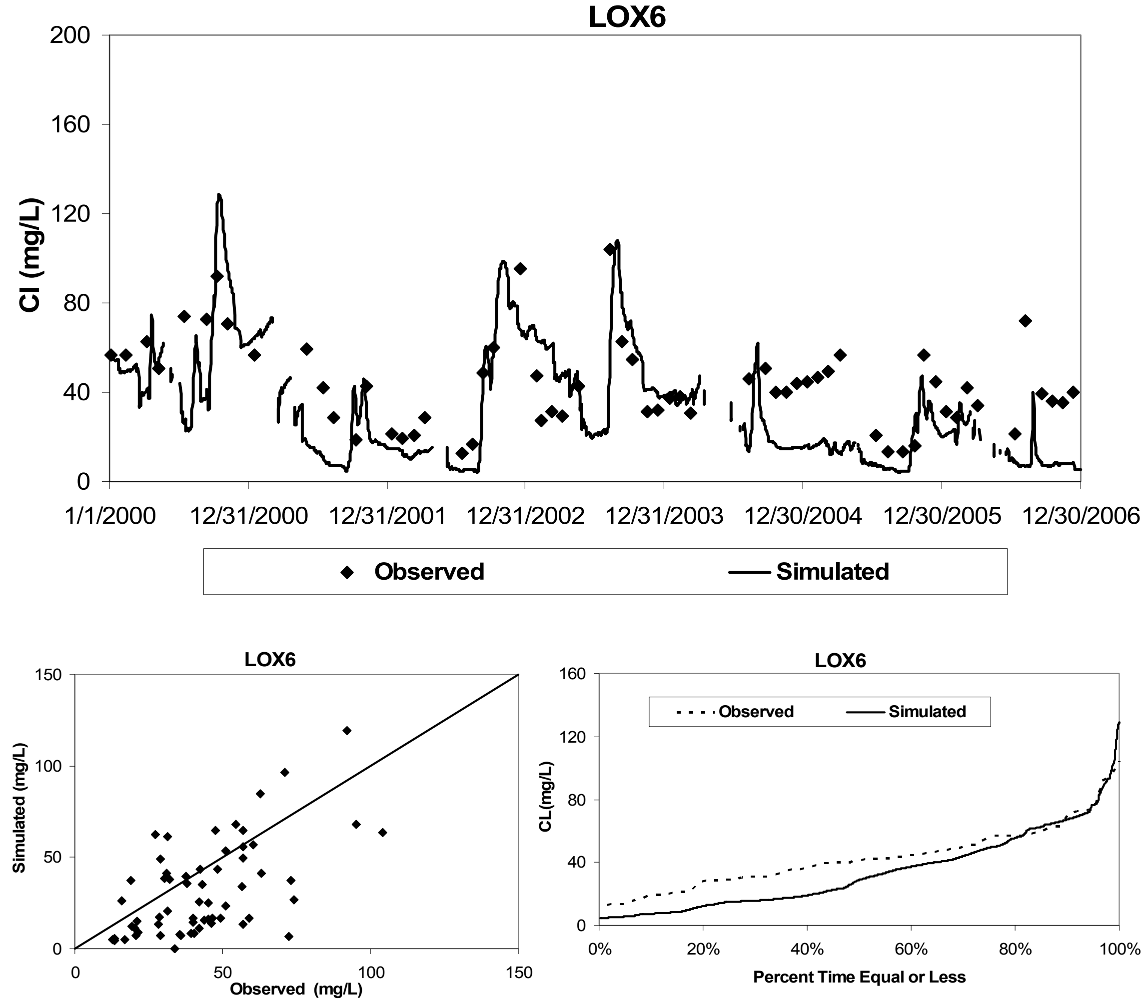
LOX6
200
160
120
80
40
0
Cl (mg/L)
1/1/2000
12/31/2000
12/31/2001
12/31/2002
12/31/2003
12/30/2004
12/30/2005
12/30/2006
Observed
Simulated
LOX6
150
100
50
0
Simulated (mg/L)
0
50
100
150
Observed (mg/L)
LOX6
160
120
80
40
0
CL(mg/L)
Observed
Simulated
0%
20%
40%
60%
80%
100%
Percent Time Equal or Less

(b)

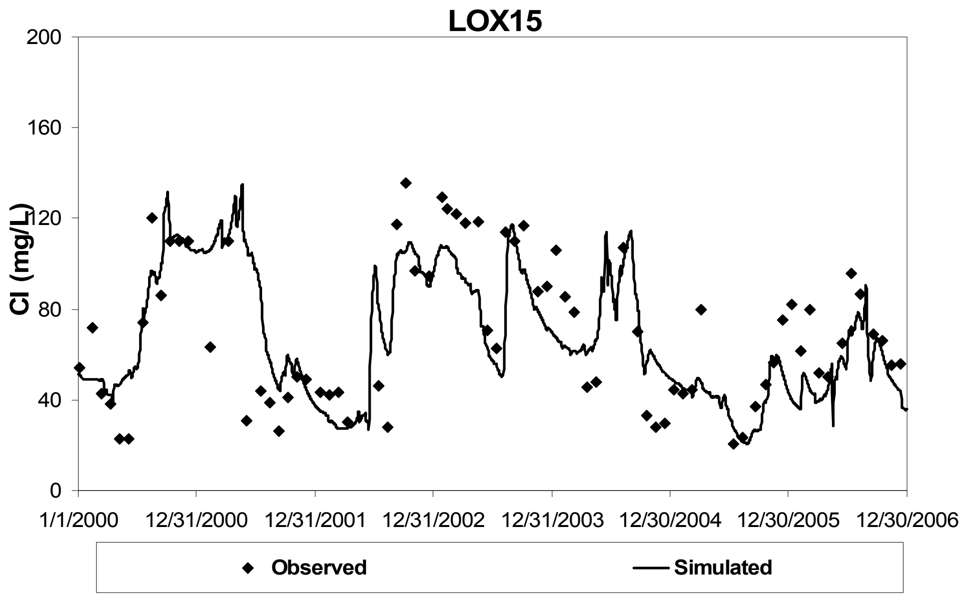
LOX15
Cl (mg/L)
200
160
120
80
40
0
1/1/2000
12/31/2000
12/31/2001
12/31/2002
12/31/2003
12/30/2004
12/30/2005
12/30/2006
Observed
Simulated

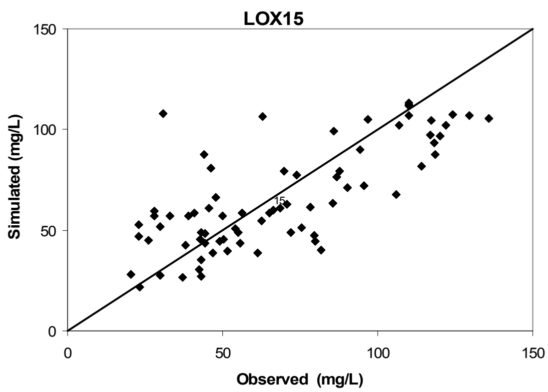
LOX15
Simulated (mg/L)
Observed (mg/L)
0
50
100
150

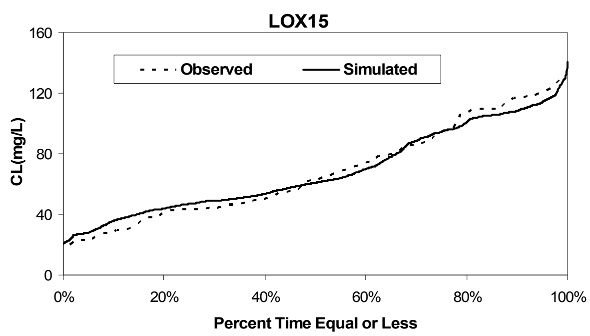
LOX15
Observed
Simulated
CL(mg/L)
0
40
80
120
160
0%
20%
40%
60%
80%
100%
Percent Time Equal or Less

(c)

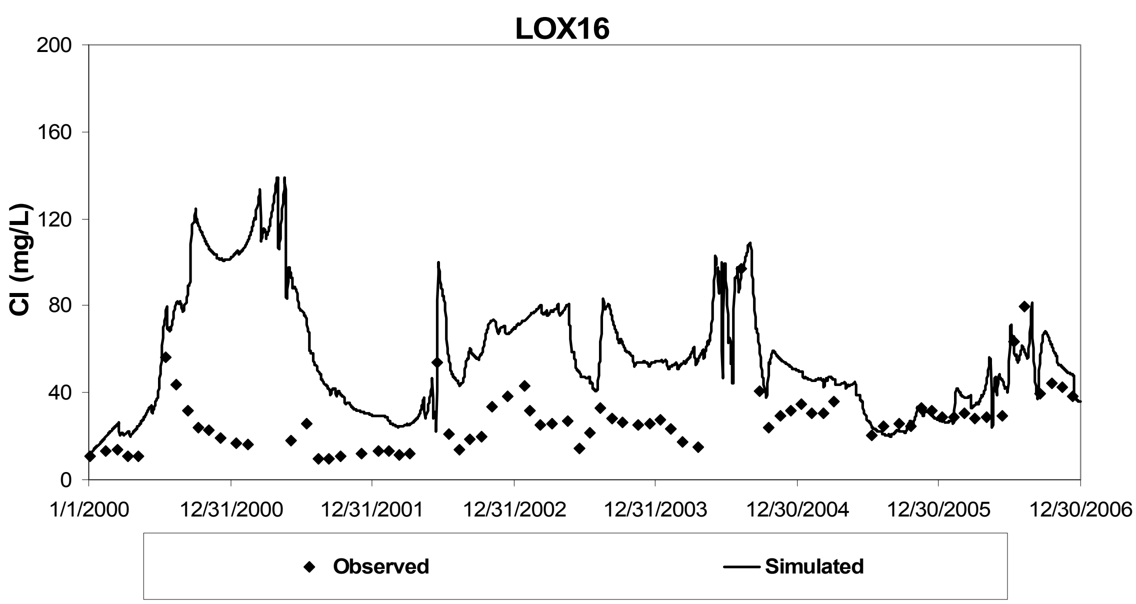
LOX16
Cl (mg/L)
200
160
120
80
40
0
1/1/2000
12/31/2000
12/31/2001
12/31/2002
12/31/2003
12/30/2004
12/30/2005
12/30/2006
Observed
Simulated

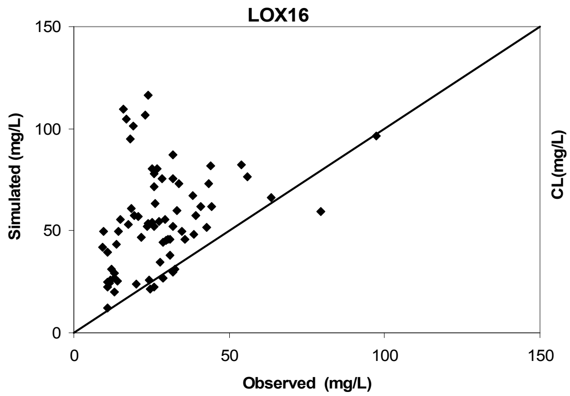
LOX16
Simulated (mg/L)
Observed (mg/L)
0
50
100
150

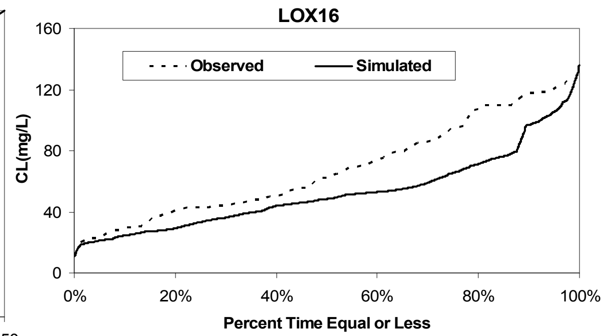
LOX16
Observed
Simulated
CL(mg/L)
Percent Time Equal or Less
0
40
80
120
160
0%
20%
40%
60%
80%
100%

(d)

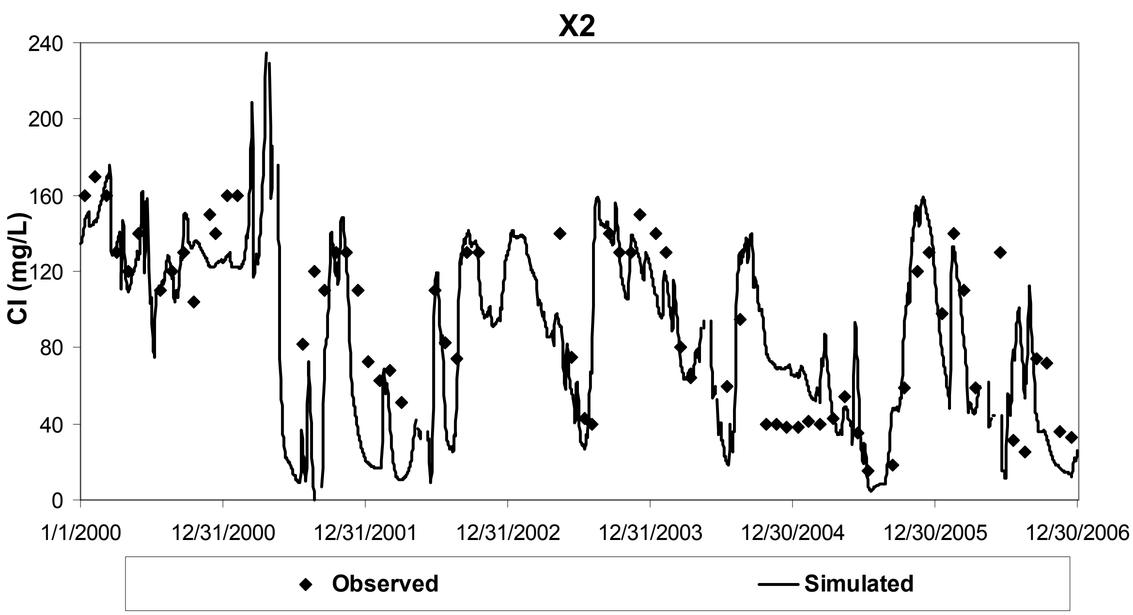
X2
Cl (mg/L)
0
40
80
120
160
200
240
1/1/2000
12/31/2000
12/31/2001
12/31/2002
12/31/2003
12/30/2004
12/30/2005
12/30/2006
Observed
Simulated

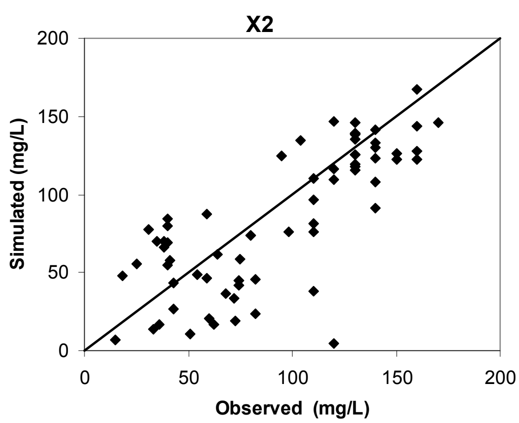
X2
Simulated (mg/L)
Observed (mg/L)
0
50
100
150
200

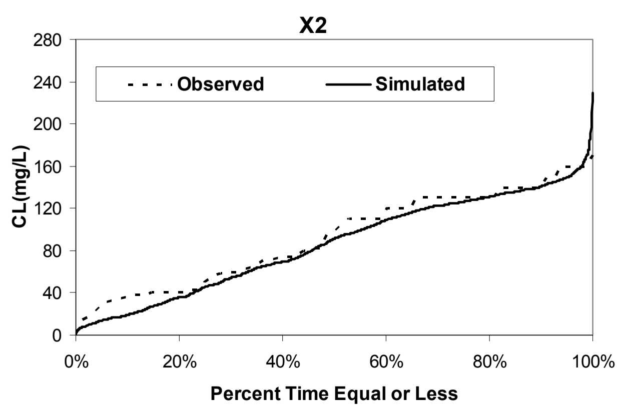
X2
Observed
Simulated
CL(mg/L)
Percent Time Equal or Less
0
40
80
120
160
200
240
280
0%
20%
40%
60%
80%
100%

(e)

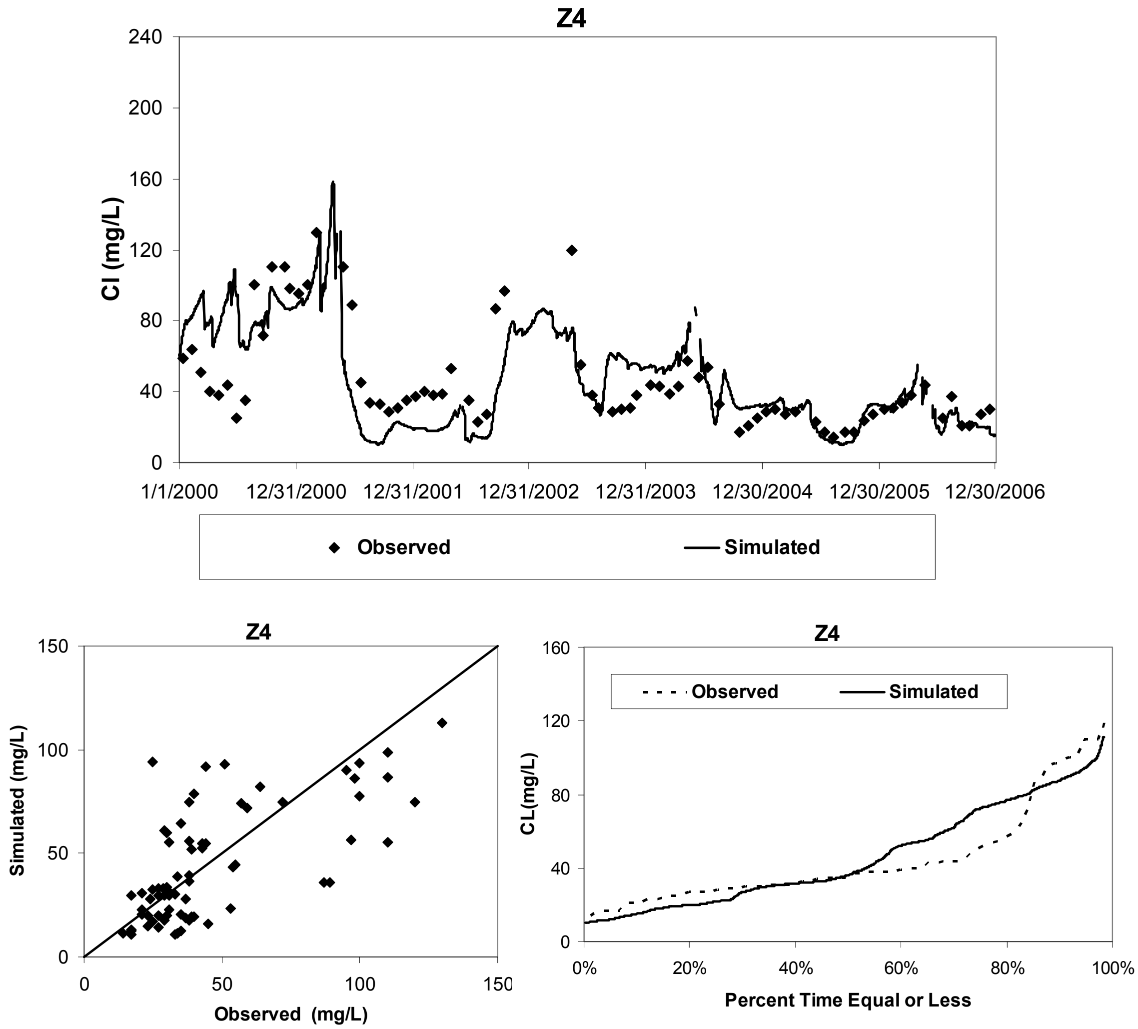
Z4
Cl (mg/L)
240
200
160
120
80
40
0
1/1/2000
12/31/2000
12/31/2001
12/31/2002
12/31/2003
12/30/2004
12/30/2005
12/30/2006
Observed
Simulated
Z4
Simulated (mg/L)
150
100
50
0
0
50
100
150
Observed (mg/L)
Z4
CL(mg/L)
160
120
80
40
0
Observed
Simulated
0%
20%
40%
60%
80%
100%
Percent Time Equal or Less

(f)

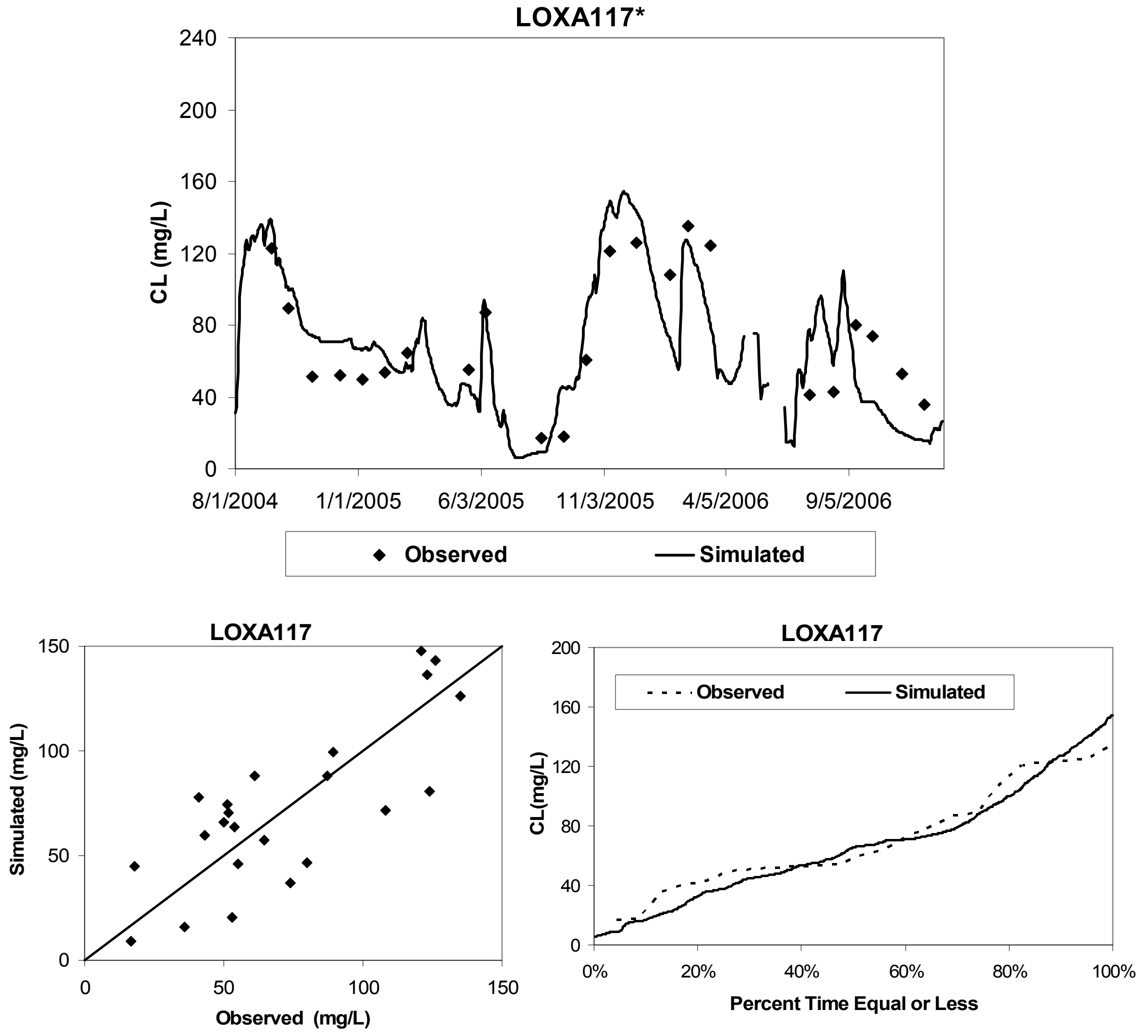
LOXA117*
240
200
160
120
80
40
0
CL (mg/L)
8/1/2004
1/1/2005
6/3/2005
11/3/2005
4/5/2006
9/5/2006
Observed
Simulated
LOXA117
150
100
50
0
Simulated (mg/L)
0
50
100
150
Observed (mg/L)
LOXA117
200
160
120
80
40
0
CL(mg/L)
Observed
Simulated
0%
20%
40%
60%
80%
100%
Percent Time Equal or Less

(g)

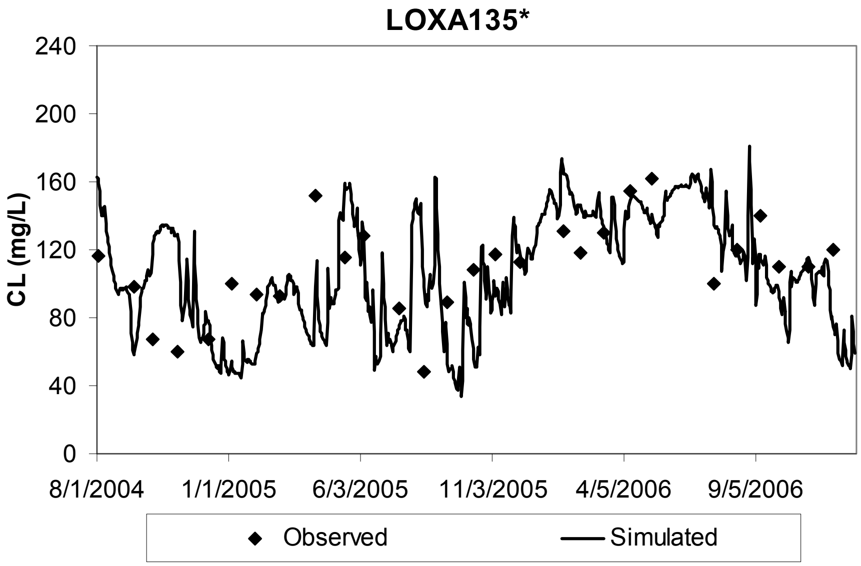
LOXA135*
240
200
160
120
80
40
0
CL (mg/L)
8/1/2004
1/1/2005
6/3/2005
11/3/2005
4/5/2006
9/5/2006
Observed
Simulated

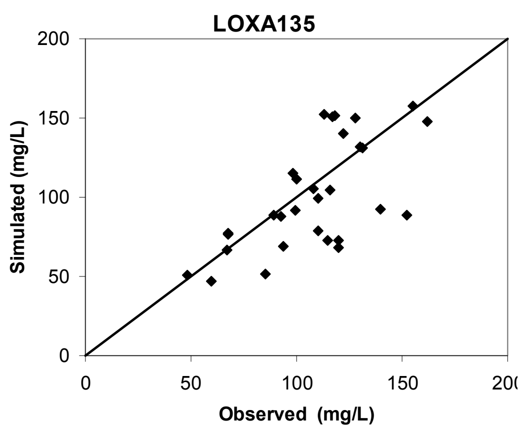
LOXA135
200
150
100
50
0
Simulated (mg/L)
0
50
100
150
200
Observed (mg/L)

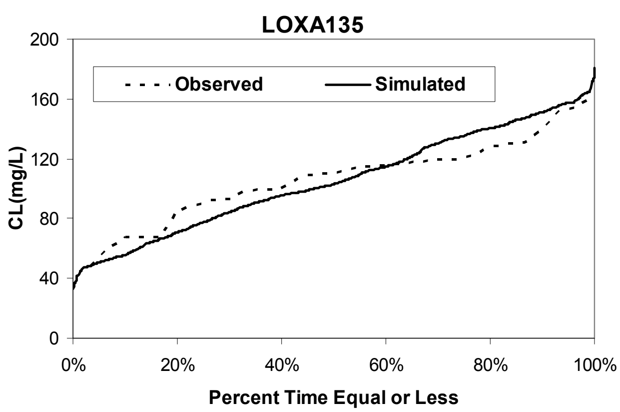
LOXA135
200
160
120
80
40
0
CL(mg/L)
Observed
Simulated
0%
20%
40%
60%
80%
100%
Percent Time Equal or Less

(h)

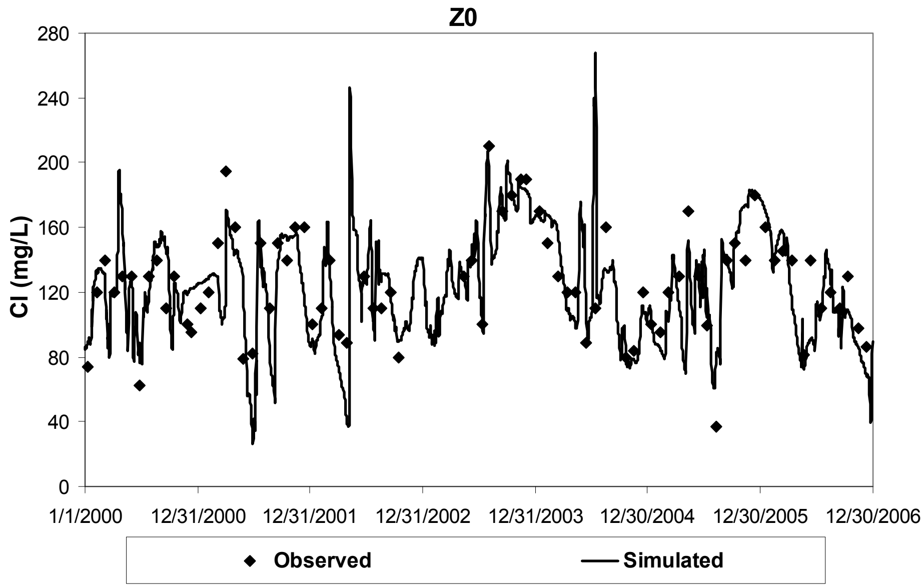
Z0
Cl (mg/L)
280
240
200
160
120
80
40
0
1/1/2000
12/31/2000
12/31/2001
12/31/2002
12/31/2003
12/30/2004
12/30/2005
12/30/2006
Observed
Simulated

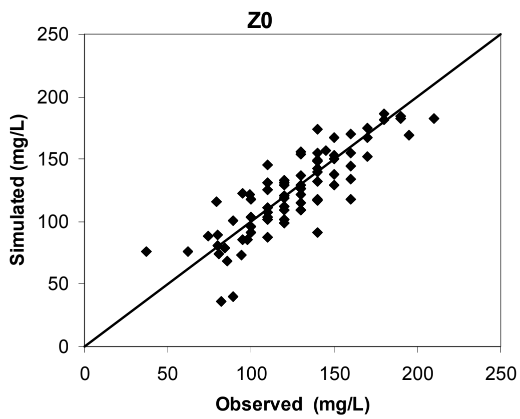
Z0
Simulated (mg/L)
Observed (mg/L)
0
50
100
150
200
250

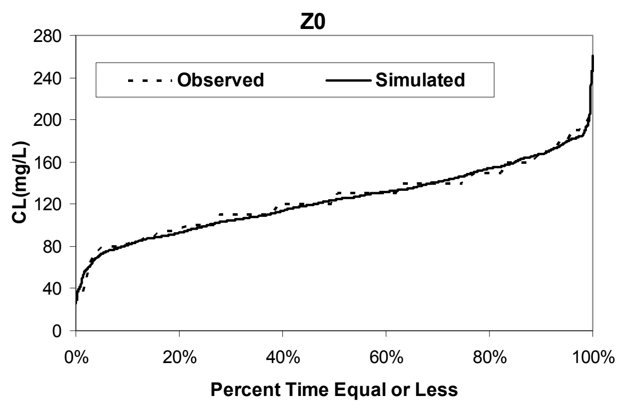
Z0
CL(mg/L)
Observed
Simulated
0%
20%
40%
60%
80%
100%
Percent Time Equal or Less

(i)

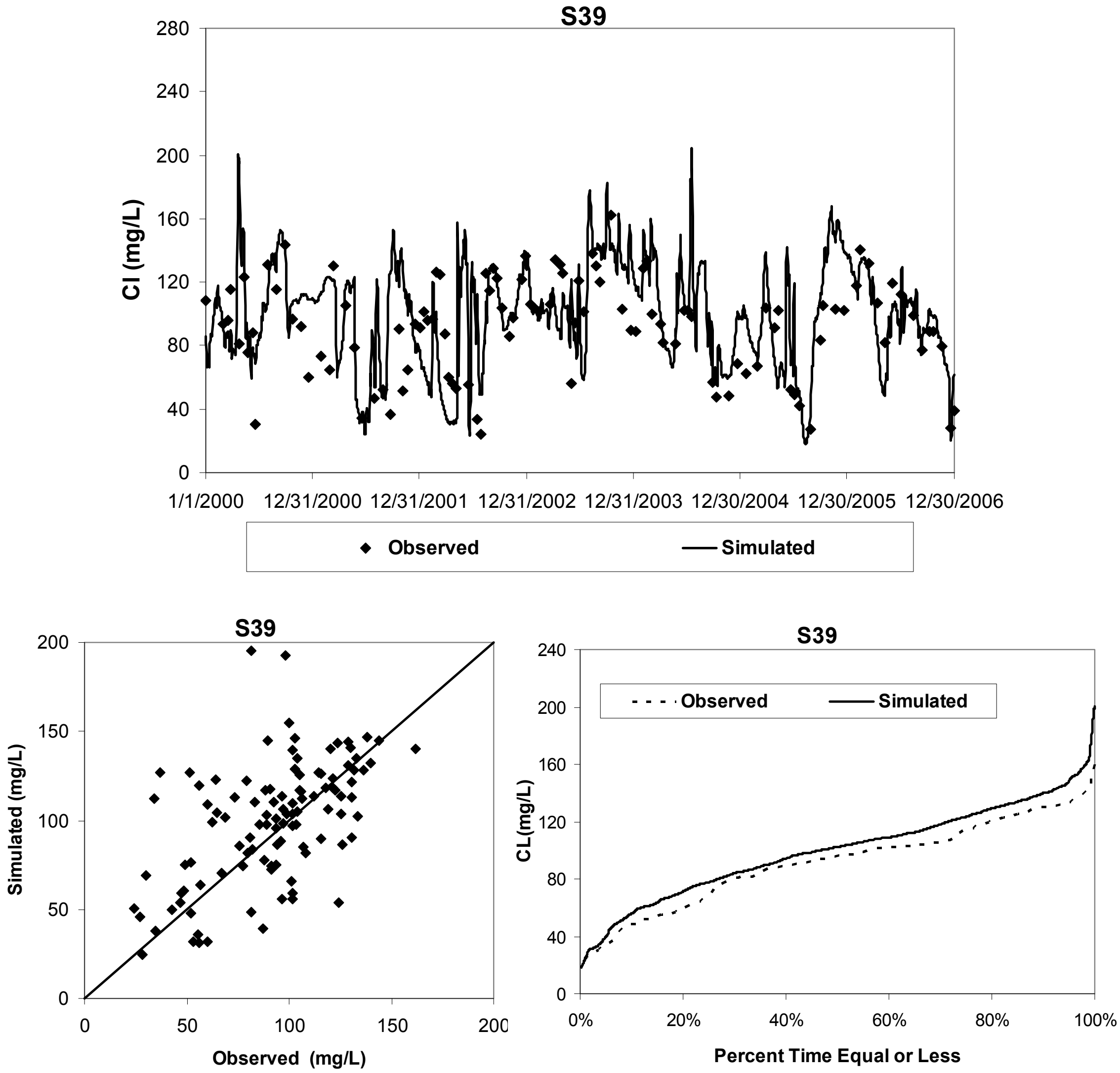

S39
Cl (mg/L)
280
240
200
160
120
80
40
0
1/1/2000
12/31/2000
12/31/2001
12/31/2002
12/31/2003
12/30/2004
12/30/2005
12/30/2006
Observed
Simulated
S39
Simulated (mg/L)
200
150
100
50
0
Observed (mg/L)
S39
CL(mg/L)
240
200
160
120
80
40
0
0%
20%
40%
60%
80%
100%
Percent Time Equal or Less
Observed
Simulated

(j)

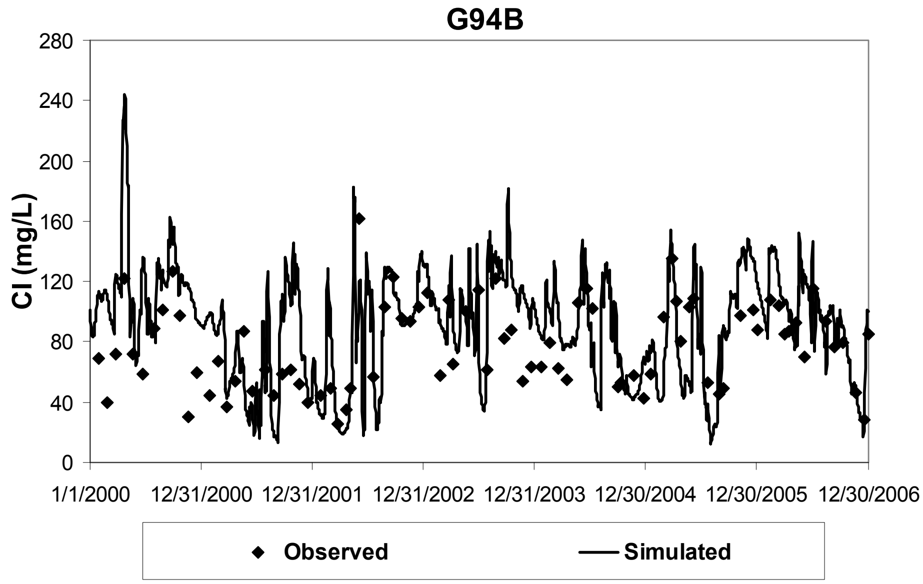

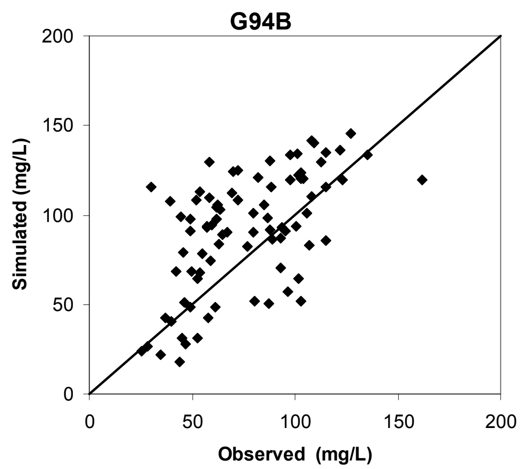

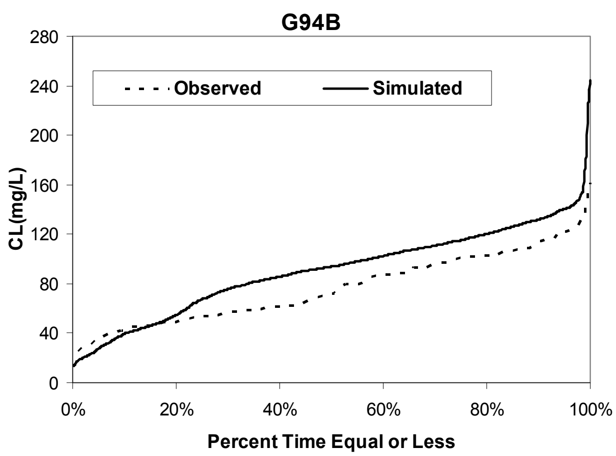

Figure 12. Comparison of Chloride concentration with measured data (including time series, scattered plot, and percentage exceedance plot) at stations of EVPA (a-c), XYZ (d-e), enhanced (f-g), and the canal station (h-j).

Table 6. Statistics of chloride concentration at selected stations for the calibration period (2000-2004)

Station	Bias (mg/L)	RMSE (mg/L)	Average Observed (mg/L)	Average Model (mg/L)	SD Observed (mg/L)	SD Model (mg/L)	SD Error (mg/L)	Variance reduction	R (Correl Coef)	r2	Nash-Sutcliffe Eff
LOX6	-5.75	25.30	49.63	42.75	25.89	27.15	24.92	0.07	0.64	0.41	0.08
LOX15	1.41	22.59	73.39	74.80	35.36	26.02	22.76	0.59	0.77	0.59	0.58
LOX16	35.85	42.33	24.72	60.57	15.19	25.74	22.73	-1.24	0.48	0.23	-6.92
X2	-16.29	34.28	107.94	91.66	38.65	46.63	30.45	0.38	0.76	0.58	0.20

Z4	-2.60	26.48	53.75	51.26	29.85	28.69	26.61	0.21	0.59	0.35	0.21
Z0	0.63	28.34	126.78	127.42	33.48	38.97	28.59	0.27	0.70	0.49	0.27
S39	7.86	34.04	93.50	101.36	30.67	34.76	33.33	-0.18	0.49	0.24	-0.25
G-94B	19.50	36.76	73.68	93.18	29.66	37.72	31.43	-0.12	0.59	0.34	-0.56

Table 7. Statistics of chloride concentration at selected stations for the validation period (2005-2006)

Station	Bias (mg/L)	RMSE (mg/L)	Average Observed (mg/L)	Average Model (mg/L)	SD Observed (mg/L)	SD Model (mg/L)	SD Error (mg/L)	Variance reduction	R (Correl Coef)	r2	Nash-Sutcliffe Eff
LOX6	-22.78	27.69	37.39	14.58	15.22	8.50	16.16	-0.13	0.25	0.06	-2.16
LOX15	-11.40	17.29	58.58	47.18	19.76	13.53	13.30	0.55	0.74	0.55	0.20
LOX16	5.75	10.94	35.19	40.94	13.40	13.74	9.52	0.50	0.75	0.57	0.30
X2	3.79	24.25	61.35	62.02	40.40	39.87	24.52	0.63	0.80	0.65	0.59
Z4	-1.11	4.98	26.89	24.96	7.49	8.96	4.98	0.56	0.84	0.70	0.41
Z0	-2.07	18.95	122.96	120.89	31.64	32.95	19.24	0.63	0.82	0.68	0.63
S39	5.97	22.38	87.04	93.01	29.78	32.63	22.00	45%	0.76	0.57	0.41
G-94B	7.72	27.17	84.59	92.32	25.26	34.46	26.56	-0.11	0.64	0.41	-0.20
LOXA109*	-4.16	21.61	41.06	36.91	24.54	25.83	21.66	22%	0.63	0.40	0.19
LOXA135*	-6.94	26.84	107.86	100.92	27.98	34.30	26.37	11%	0.66	0.43	0.05

Note: * indicates that the data for the Enhanced stations started from August 2004. The statistics are calculated for the period from the date when the data become available to the end of 2006.

The overall model predictions compared well with the observed data range both for the marsh and the canal stations. We believe that a major cause of errors in chloride projections can be linked to inadequacy of sampling at the canal inflows. Inflow sampling for chloride was performed by grab sampling approximately every two weeks. Chloride concentration was variable and showed some dependence on discharge. Thus, more frequent, or flow proportional sampling was needed to adequately characterize chloride inflow loads; increased sampling frequency or deployment of sondes to log conductivity as a surrogate for chloride concentration at the inflows would address this data need. This improved monitoring would significantly improve model performance. Other sources of uncertainty that impacted the model performance include the estimated dry and wet deposition rates of chloride and the inadequate resolution of topographic data for the Refuge.

To elucidate the impacts of canal water intrusion, concentration profiles along two transects around the XYZ stations were extracted. The X-transect includes stations X0, X1, X2, X3, and X4; and the Z-transect includes stations Z0, Z1, Z2, Z3, Z4, and LOX12. Figure 13 shows the comparisons of observed concentration and profiles of model results for two intrusion events occurred in 2000 and 2002, respectively. The field measurements used in the profiles were gathered at different times. Therefore, model results were extracted over a time period enveloping the duration over which the field data was gathered. A four-week window around the field measurements proved sufficient to capture the intrusion event. In general, the concentration gradient pattern was reproduced by the model. The elevated concentration observed from the transitional zone towards the interior marsh indicates that there is substantial canal water intrusion extending a few kilometers into the marsh. The modeled concentration, in general, declines more rapidly along canal-marsh transects than is observed. This may result from inadequate vegetation and topographic data to adequately describe the zone across peripheral marsh to the canal levee.

(a)

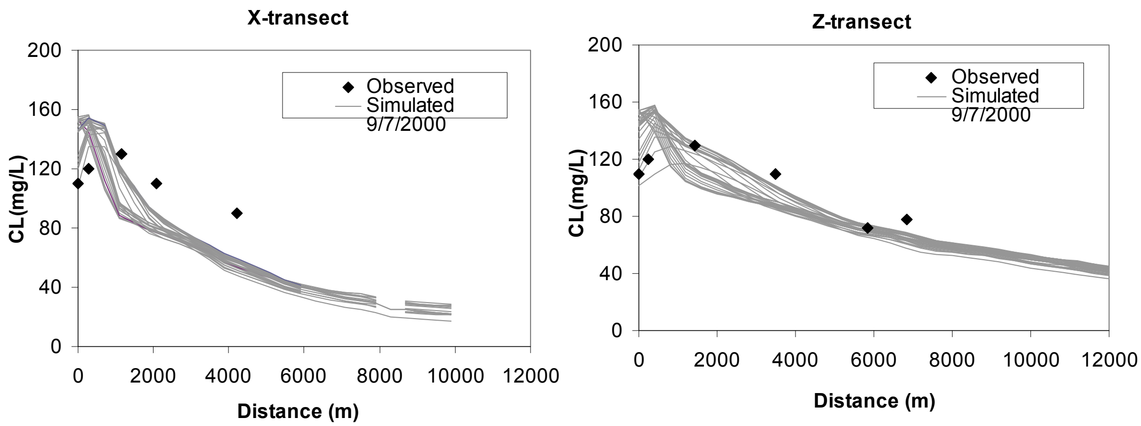

(b)

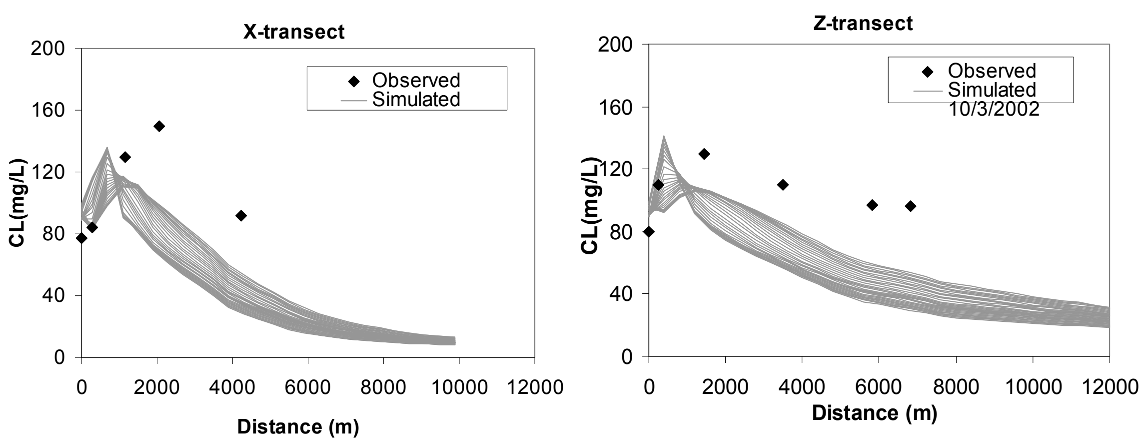

Figure 13. Chloride concentration of measured and extracted profiles along the X and Z transects with a two-week window before and after the measurement (a) event of 9/20/2000 (window 9/6/2000-10/4/2000) (b) event of 10/15/2002 (window10/2/2002-10/29/2002).

6.4 Management Scenarios

It is essential for the Refuge to have the capability of assessing and comparing alternative water management operational plans and alternative structures. The calibrated and validated model provides this capability. Additionally, a better understanding of the hydrologic and water quality process affecting the Refuge can be gained through application of hypothetical scenarios. Herein, two scenarios were examined. Scenario 1 quantifies the importance of chloride loading from inflows on Refuge chloride levels (the completely rainfall-driven test scenario). Scenario 2 illustrates the preliminary analysis of the impact of a hypothetical project designed to block overbank flow along the eastern canal (the berm scenario).

Scenario 1: The chloride concentrations at all the inflow structures along the length of the rim canal were reduced to a constant 2 mg/L, a value equal to the concentration assumed in wet atmospheric deposition. This modeling experiment examined the influence of the chloride loading from the inflow structures on the marsh interior. The comparison of concentration for the original boundary concentration (referred to herein as the "Base" conditions) and the reduced inflow concentration (2 mg/L) provided a visualization of the residence time of water in the marsh and canal systems as both models use the same initial concentration (Figure 14). The residence time at the selected marsh sites (Figure 14a-b) was equal to or greater than one year, but the canal (Figure 14c) initially responded much more rapidly, while continued to respond as chloride flows from the marsh. This scenario also quantified the concentrating of chloride through evaporation (a distillation process) by simulating marsh that is no longer impacted by canal water intrusion. During the dry season, when ET and seepage exceed precipitation, the chloride concentration increased and at times reached as high as 12.5 mg/L for LOX10 and 18.6 mg/L for LOX11. When the wet season started, the rainfall diluted the concentration, but most marsh stations remain over 3 mg/L. Evaporation therefore concentrated chloride by a factor of 1.5 to nearly 10 at more isolated interior marsh sites like LOX11. Although the concentrating effect of evaporation does at times significantly raise modeled chloride concentrations, comparison to base run concentrations at these sites illustrate that most of the chloride mass at interior sites originates at pumped inflows rather than in aerial deposition.

(a)

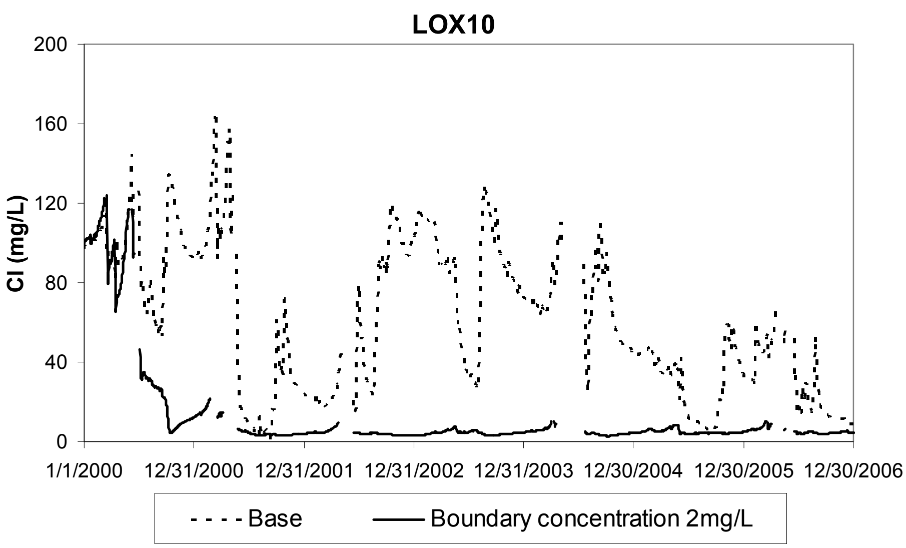

(b)

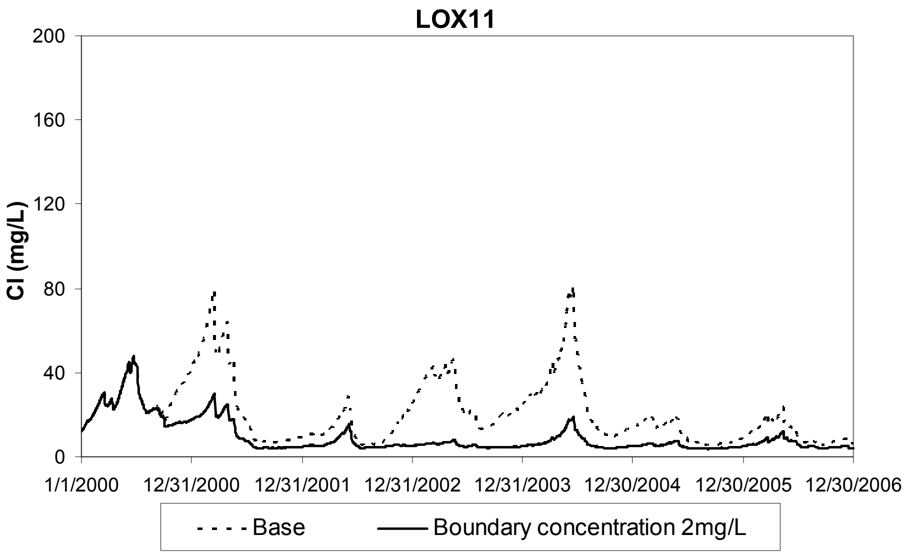

(c)

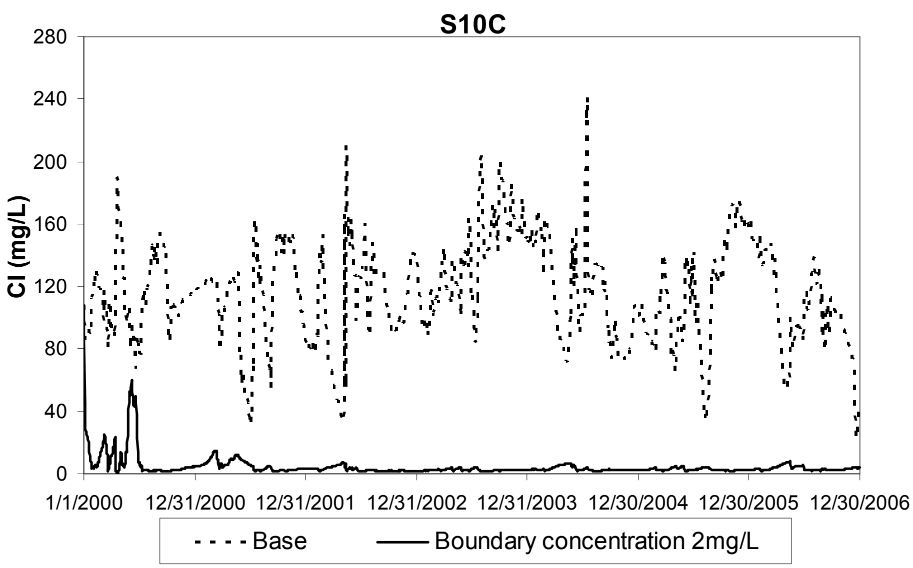

Figure 14. Comparison of Chloride concentration with original boundary inflow concentration (Base) and reduced concentration (2 mg/L, same as rainfall concentration) at marsh stations (a-b) and canal station (c).

Scenario 2: At times, water for water supply use is routed through the eastern Refuge L-40 Canal for delivery to users east and southeast of the Refuge. It has been proposed (SFWMD, 2005b) that it would be beneficial to greatly reduce or eliminate contact and mixing between the water from the eastern canal and the marsh because that would reduce marsh nutrient and mineral concentration, and might avoid unnecessarily treating water that is simply being routed to water supply structures. Before this proposal can be considered further, there is a need to perform a preliminary analysis of impacts on hydrology and canal-marsh exchange. In this scenario, a hypothetical berm is built along the eastern canal. The berm was modeled by simply removing the links between the canal and marsh along the entire length of the eastern canal. The comparisons of stage and concentration at several stations between the base conditions (without berm) and with berm are given in Figure 5.

(a)

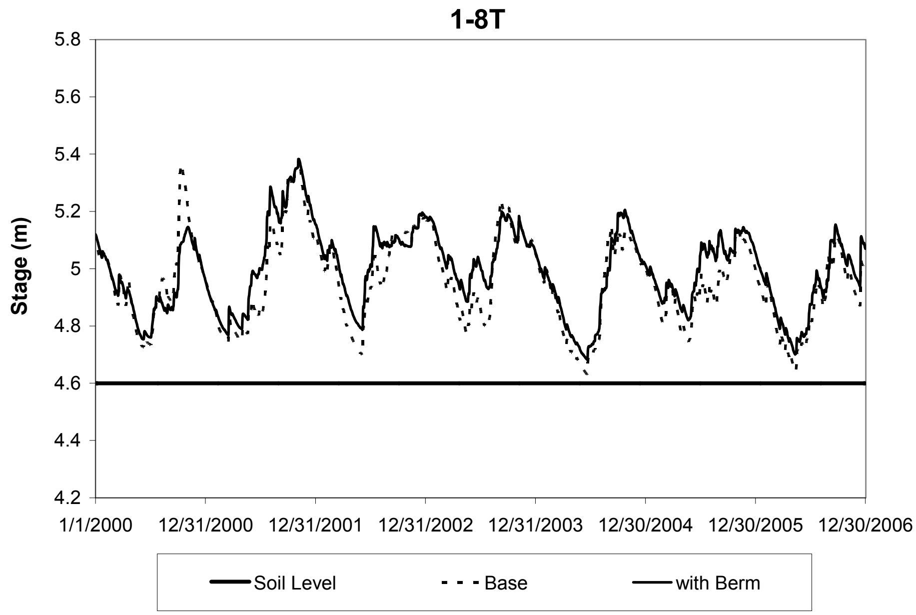

(b)

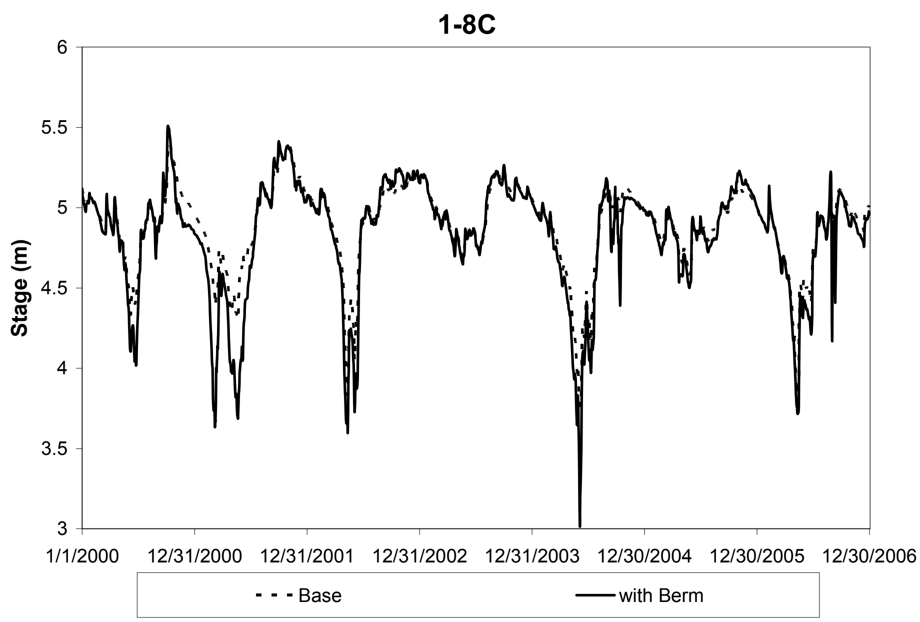

(c)

(d)

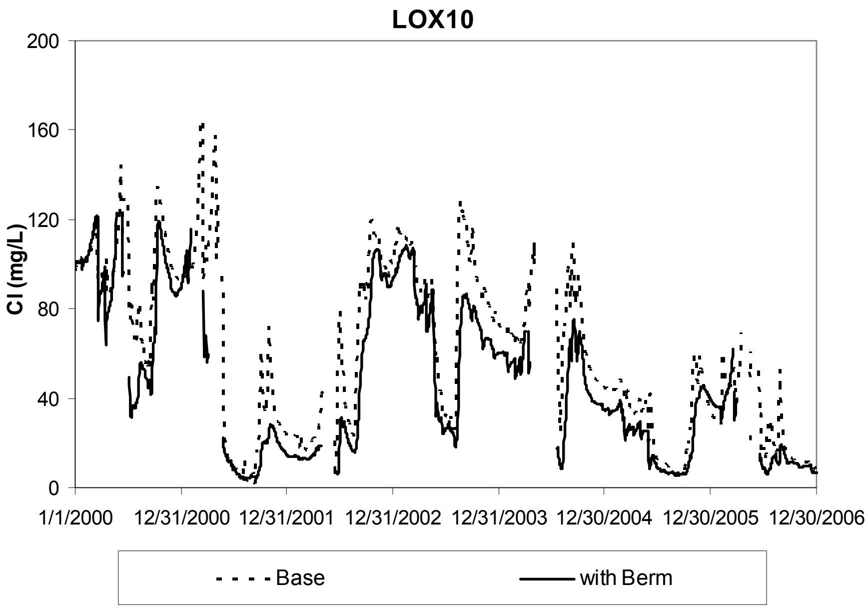
LOX10
200
160
120
80
40
0
Cl (mg/L)
1/1/2000
12/31/2000
12/31/2001
12/31/2002
12/31/2003
12/30/2004
12/30/2005
12/30/2006
Base
with Berm

(e)

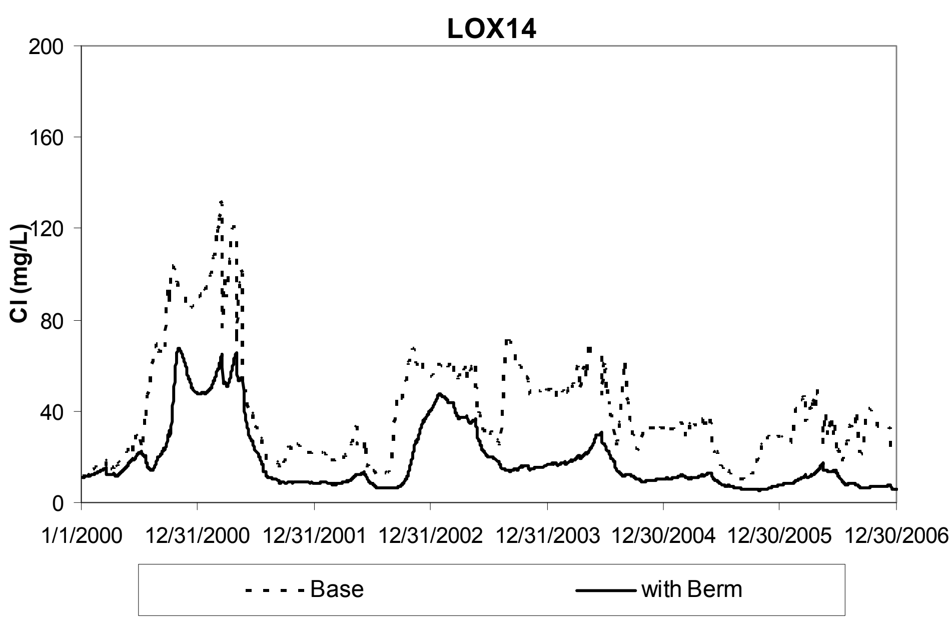
LOX14
200
160
120
80
40
0
Cl (mg/L)
1/1/2000
12/31/2000
12/31/2001
12/31/2002
12/31/2003
12/30/2004
12/30/2005
12/30/2006
Base
with Berm

(f)

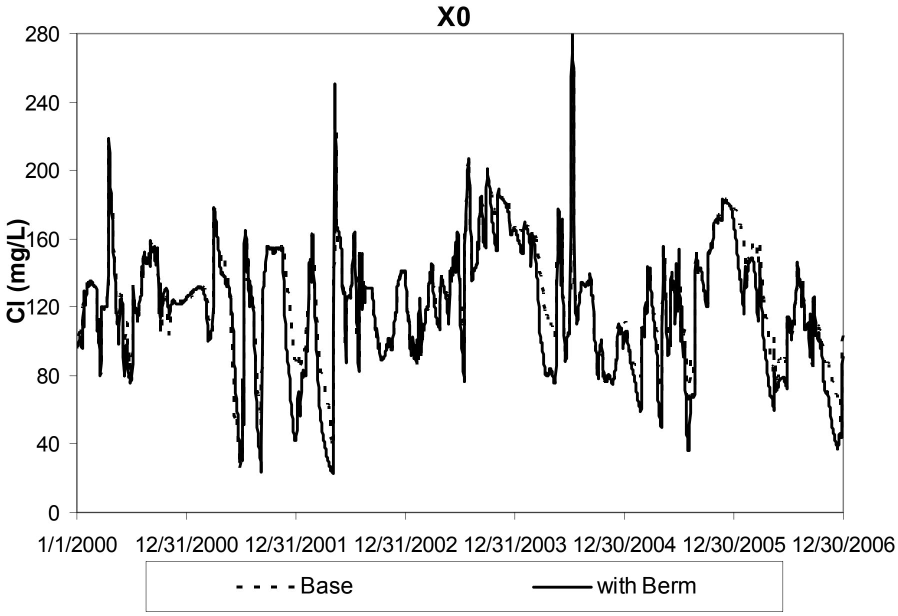
X0
280
240
200
160
120
80
40
0
Cl (mg/L)
1/1/2000
12/31/2000
12/31/2001
12/31/2002
12/31/2003
12/30/2004
12/30/2005
12/30/2006
Base
with Berm

(g)

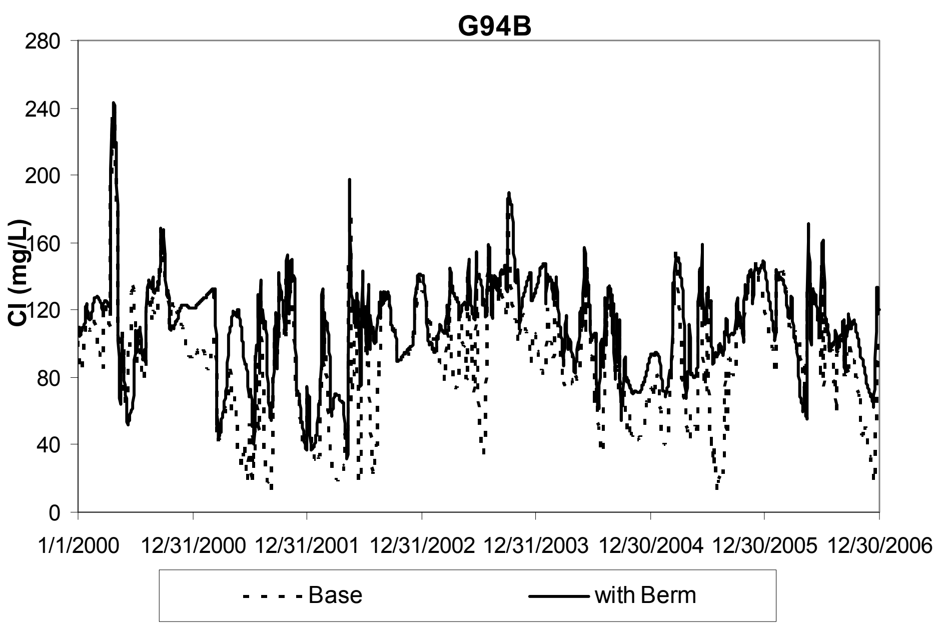
G94B
280
240
200
160
120
80
40
0
Cl (mg/L)
1/1/2000
12/31/2000
12/31/2001
12/31/2002
12/31/2003
12/30/2004
12/30/2005
12/30/2006
Base
with Berm

Figure 15. Comparison of stage (a-b) and Chloride concentration (c-g) without berm (Base) and with berm.

The Refuge's WRS primarily uses the stage measured in the eastern (L-40) canal to require regulatory water releases. When pumped inflows discharge into the L-40 canal, a transient local water accumulation and stage rise occurs that may result in additional regulatory discharge. The resultant effect is that the canal water was drained faster, which leads to a slightly lower stage than the base conditions (as seen at station 1-8C). Minor operational changes could be used in the future to reduce this excessive regulatory release. The water stage in the easternmost region of the marsh (represented by station 1-8T) increased as rain water could not be drained to the eastern canal.

Blockage of the marsh flow to the eastern canal caused the chloride concentration in the eastern canal to increase (e.g., G-94B). The effect of constructing the berm on the western canal is not as pronounced. The chloride concentrations decreased slightly (as seen at station X0). The decrease can be a result of the additional runoff from the marsh interior (carrying low chloride concentration) that typically would have drained to the eastern canal. For the marsh interior the chloride concentration was drastically reduced in the eastern side (LOX6 and LOX14) due to the protection from the eastern canal water intrusion events, while only slightly reduced in the western marsh (LOX10). Based on our model simulations, we project that with the berm in place, canal water of higher concentration would be directed south down the eastern canal, and substantially reduce high concentration canal water from penetrating into the Refuge. This analysis focused on characterizing hydrology and canal-marsh dynamics related to a berm. It is important to note that no ecological or other analyses were conducted. This analysis demonstrates a potential for a water quality benefit from physically barring water penetration into the marsh, but any management decision to support such an extensive and intrusive structure would require further detailed consideration and design to quantify the multiple direct and indirect wetland impacts and benefits of alternatives.

7. Discussion

During calibration, previous hydrological models of the Refuge used historical flow records to define not only the inflow, but also the outflow flow boundary (SFWMD, 2005a). Using only historic outflow for calibration is straightforward and would be anticipated to provide good calibration results. However, this approach does not provide a test of the rule-based outflow management that is necessary when testing scenarios that do not apply the historic inflow time series. Our study simulated regulatory outflows triggered by stages higher than a seasonally variable regulation schedule, and used historical flows for water supply and storm-forecast related outflows. Decisions on regulatory water releases from the Refuge often depend partially on information unavailable within the Refuge model (stages downstream, weather forecasts, and water supply needs), as well as professional judgment of water managers. Thus, any model of regulatory outflow operations is challenging, will not precisely reproduce historic values, and should be tested before being used in analyses involving changes in Refuge inflows and outflows (Arceneaux et al., 2007). In our approach, historic structure outflow then provides an additional calibration test through comparison with modeled outflows, and calibration results demonstrate that our stage-discharge relationship is credible.

Calibration shows that stage is relatively insensitive to certain hydrologic parameters, such as canal and marsh roughness, and dry and wet depths. Site-specific velocity and patterns of mass transport, however, are sensitive to these parameters. One could use velocity measurements as added calibration criteria to augment the stage calibration criteria, but such measurements were unavailable in the canal or marsh to apply to model calibration. Indeed, velocity measurements of adequate spatial and temporal resolution are technically challenging and expensive, particularly in the spatially heterogeneous marsh system. Because of the conservative nature of chloride, inclusion of this constituent into the model calibration provides an alternative to evaluate the adequacy of model predicted flows.

Chloride was found to be sensitive to both dispersion and roughness, but exhibited quite different spatial patterns of sensitivity. Chloride was found to be more sensitive to dispersion in the interior marsh than in the peripheral marsh. This can be explained because velocity in the interior is low, and chloride is transported mainly by dispersion compared to the peripheral zone where transport is dominated by advection. Inversely, roughness plays a more important role in the peripheral marsh because of the relatively higher velocities and advective transport.

Literature survey reveals that dispersion in large wetland systems is not well studied. In surface water modeling, the dispersion coefficient can vary over 11 orders of magnitude, ranging from 10^{-5} cm^2/s for molecular diffusion to well over 100 m^2/s for some cases of dispersion in open estuaries (Bowie et al., 1985). In our calibration, it was found that dispersion in the central area of the marsh wetland was best characterized by a dispersion coefficient of 2 m^2/s. Although this is below values typically estimated in open-water, it is more than an order-of-magnitude above the dispersion measured in laboratory flume studies with flow around simulated emergent plant stems (Nepf et al., 1997; Lightbody and Nepf, 2006). This result suggests that dispersion modeled here largely results from the heterogeneity of flow paths and velocities that exist in this natural wetland, and suggests that stagnant zones (dead zones) and short circuiting along sloughs and boat trails may play a similarly significant role in affecting dispersion in a natural wetland as it does in constructed wetland treatment systems (Martinez and Wise, 2003; Paudel et al., 2010).

The 400 m grid currently employed in the model is the best resolution currently available to the Refuge, but still restrains the model performance in fully capturing some events. It does not capture the sloughs or other topographic features that may impact circulation patterns within the marsh interior. Further, this survey does not capture microtopographic features that likely become control flows at shallow depths. Modeling (Min and Wise, 2009) demonstrated that small scale topographic variation can have a large impact on mixing and dispersion. The importance of local site-specific conditions was illustrated in this study by sampling sites LOX15 and LOX16. Although these stations are at a similar distance to the canal and are close to each other, they at times display a considerable divergence in chloride concentration. From a modeling perspective, it appears that station LOX16 is somehow isolated from canal water carrying high chloride concentrations by topographic or vegetative features that were not captured in the topographic or vegetation surveys, and thus not properly reflected in the model. As also demonstrated by the discrepancy in modeled water depth for geographically close stations of LOXA130 and LOXA131 (Figure 10), it is believed that certain areas in the marsh interior are more protected or exposed by local features. As with all models, this model must be interpreted with an understanding of the uncertainty introduced by local topography and other local conditions beyond the resolution of the model input data.

8. Conclusions

We demonstrated that the MIKE FLOOD program which dynamically links a 1-D channel model with a 2-D rectangular grid overland flow model provides a useful platform for simulation of the hydrology of a large coupled canal and marsh system. The user programmable ECO Lab module provides a practical tool for constituent simulation, and provided considerably greater flexibility of model structure definition when compared to solely using the advection-dispersion module available in MIKE FLOOD. The graphical and statistical analysis of model performance using observed water levels, water depths, discharge, and chloride concentrations demonstrates that this model typically provides good projections of the Refuge hydrodynamics and chloride concentration that result from inflows and outflows over long and short terms. The model provides a useful tool for better understanding the causes of canal water intrusion into the marsh, and supplements analyses based solely on monitoring (Harwell et al., 2008; Surratt et al., 2008). Previous applications of this software focused on rivers, lakes, and estuaries (Patro and Chatterjee, 2009; Miller and Meselhe, 2008). To the authors' knowledge, the MIKE FLOOD modeling of a spatially expansive wetland presented here is unique. As the MIKE FLOOD model structure is capable of simulating large-scale coupled stream-wetland systems, it provides a spatial and temporal resolution that is adequate to credibly support many Refuge management decisions concerning water quality and quantity.

In order to model alternative scenarios that may alter inflows or stages within the Refuge, it is necessary to model discharges related to the WRS. In contrast to previous hydrologic modeling of the Refuge, we chose to simulate stage regulation under the Refuge WRS, rather than use historic outflows as boundary time series in calibration and validation. Here, our model calibration and validation test credibility of our model of stage management decision-making as well as the hydrological model. In our approach, modeled regulatory discharges are compared with historical values to assess adequacy of the model.

Calibration to the changing pattern of chloride in the canal and marsh did constrain the model calibration and improved the credibility of the hydrodynamic calibration of water flow. The model also provides a calibrated modeling base for future development of reactive constituents such as total phosphorus and sulfate. Although some specific data limitations were identified with regard to the quality of input data, the Refuge is data-rich and has potential for use as a prototypical system for the testing and development of future wetland models.

Applications presented here illustrate the potential value of modeling to contribute to both the understanding of large wetland ecosystems, as well as management of those systems. The interior marsh of the Refuge has often been termed rainfall driven, implying that interior water chemistry is not significantly impacted by the pumped stormwater which discharges into the canals. It was shown here that even at relatively isolated interior sites (LOX11), chloride concentration is highly sensitive to inflow chloride loading.

Even when using well-tested software, it is important to test simple mass and volume balance in model output. We found mass balance anomalies in some options including lateral links between the MIKE 11 and MIKE 21 models, and in one complex structure definition. Version 1 of the Refuge model used lateral links to couple the MIKE 11 canal model with the MIKE 21 model of the marsh. Version 1 simulated stage and discharge well, and tests showed the model conserved water volume. However, mass balance analysis of chloride demonstrated that Mike Flood lateral links do not adequately conserve constituent mass. Version 2 of the model used standard links to simulate exchange between the MIKE 21 marsh model and the MIKE 11 canal model. Version 2 does adequately conserve water and mass. However, mass balance error is detectable, and results from the MIKE 21 implementation of modeling drying and wetting cycles. This error is directly associated with the wet/dry switching frequency and the number of cells involved in the switches. Therefore, the model is more applicable for simulating periods when the cells are typically wet.

Alternative model definitions were developed to obviate use of problematic MIKE FLOOD options. Our experience illustrates the importance of users testing model definitions using simplified examples, professional judgment, and overall mass and volume budget testing. We conclude that this model can provide a valuable management tool supporting alternative analysis and operational decisions within the Refuge. An analogous approach should similarly prove to be of value in management of other Everglades wetlands, and in large wetland systems throughout the world.

References

Alvord, H.H., Kadlec, R.H., 1996. Atrazine fate and transport in the Des Plaines wetlands. Ecological Modeling 90 (1), 97-107.

Andersen, J., Refsgaard, J.C., and Jensen, K.H., 2001. Distributed hydrological modeling of the Senegal river basin—model construction and validation. Journal of Hydrology 247, 200-214.

Ansar, M., Chen, Z., 2009. Generalized flow rating equations at prototype gated spillways. Journal of Hydraulic Engineering 135(7), 602-608.

Arceneaux, J., Meselhe, E.A., Griborio, A., Waldon, M.G., 2007. The Arthur R. Marshall Loxahatchee National Wildlife Refuge Water Budget and Water Quality Models. Report No. LOXA-07-004, currently available at < http://loxmodel.mwaldon.com >, University of Louisiana at Lafayette in cooperation with the U.S. Fish and Wildlife Service, Lafayette, Louisiana.

Bowie, G.L., Mills, W.B., Porcella, C.B., Campbell, C.L., Pagenkopf, J.R., Rupp, G.L., Johnson, K.M., Chan, P.W.H., Gherini, S.A., 1985. Rates, Constants, and Kinetic Formulations in Water Quality Modeling (Second Edition). EPA/600/3-85/040, USEPA Environmental Research Lab, Athens, Georgia.

Brandt, L.A., 2006. Benefits Anticipated from the 1995 Water Regulation Schedule for Water Conservation Area 1: Review and Analysis. Report No. LOXA06-006, available at < http://sofia.usgs.gov/publications/reports/wca1_review/ >, U.S. Fish and Wildlife Service, Boynton Beach, FL.

Brandt, L.A., Portier, K.M., Kitchens, W.M., 2000. Patterns of change in tree islands in Arthur R. Marshall Loxahatchee National Wildlife Refuge from 1950 to 1991. Wetlands 20 (1), 1-14.

Browder, J.A., Gleason, P.J., Swift, D.R., 1991. Periphyton in the Everglades: spatial variation, environmental correlates, and ecological implications. In: Davis, S.M., Ogden, J.C. (Eds.). Proceedings of Everglades Symposium, Key Largo, FL 1989, 76pp. <http://mwaldon.com/Loxahatchee/GrayLiterature/Browder-et-al-1991.pdf>.

Browder, J.A., Gleason, P.J., Swift, D.R., 1994. Periphyton in the Everglades: spatial variation, environmental correlates, and ecological implications. In: Davis, S.M., Ogden, J.C. (Eds.). Everglades: The Ecosystem and its Restoration. St. Lucie Press, Boca Raton, FL, Ch. 16, 379-418.

Daroub, S., Stuck, J.D., Rice, R.W., Lang, T.A., Diaz, O.A., 2002. Implementation and verification of BMPs for reducing P loading in the EAA and Everglades Agricultural Area BMPs for reducing particulate phosphorus transport. Phase 10 annual report. WM 754, Everglades Research and Education Center, Institute of Food and Agricultural Sciences, University of Florida, Belle Glade, FL.

Desmond, G., 2003. South Florida high-accuracy elevation data collection project. FS-162-96, U.S. Department of the Interior, U.S. Geological Survey, Reston, VA. < http://sofia.usgs.gov/publications/fs/162-96/ >.

DHI Water & Environment, 2008d. MIKE 21 FLOW MODEL, Advectio/Dispersion Module: User Guide. Hørsholm, Denmark. <http://www.dhigroup.com/>.

Gilvear, D.J., Bradley, C., 2000. Hydrological monitoring and surveillance for wetland conservation and management; a UK perspective. Physics and Chemistry of the Earth (B) 25 (7–8), 571–588.

Harwell, M.C., Surratt, D.D., Barone, D.M., Aumen, N.G., 2008. Conductivity as a tracer of agricultural and urban runoff to delineate water quality impacts in the northern Everglades. Environmental Monitoring and Assessment 147, 445-462.

Hollis, G.E., Thompson, J.R., 1998. Hydrological data for wetland management. Journal of the Chartered Institution of Water and Environmental Management 12, 9–17.

Kadlec, R.H., Hammer, D.E., 1988. Modeling nutrient behavior in wetlands. Ecological Modeling 40, 37-66.

Kadlec, R.H., Knight, R.L., 1996. Treatment Wetlands. CRC Lewis Publishers, Boca Raton, FL, 934 pp.

Koskiaho, J., 2003. Flow velocity retardation and sediment retention in two constructed wetland-ponds. Ecological Engineering 19 (5), 325-337.

Lightbody, A.F., Nepf, H.M., 2006. Prediction of velocity profiles and longitudinal dispersion in emergent salt marsh vegetation. Limnology and Oceanography 51 (1), 218-228.

Mackay, D., Paterson, S., Shiu, W.Y., 1992. Generic models for evaluating the regional fate of chemicals. Chemosphere 24 (6), 695–717.

Martinez, C. J., and Wise, W. R. (2003). "Hydraulic Analysis of Orlando Easterly Wetland." Journal of Environmental Engineering, 129(6), 553-560.

Martin, J.F., Reddy, K.R., 1991. Modeling nutrient retention of freshwater coastal wetland: estimating the roles of primary productivity sedimentation, resuspension and hydrology. Ecological Modeling 54, 151–187.

McCormick, P., Crawford, E.S., 2006. Vegetation responses to mineral gradients in an ombrotrophic northern Everglades peatland, the Arthur R. Marshall Loxahatchee National Wildlife Refuge. Greater Everglades Ecosystem Restoration Conference, Orlando, FL.

Meselhe, E.A., Arceneaux, J., Waldon, M.G., 2007. Mass balance model version 1.01. LOXA-07-002, University of Louisiana - Lafayette in cooperation with the U.S. Fish and Wildlife Service, Lafayette, LA. <http://loxmodel.mwaldon.com >.

Meselhe, E.A., Griborio, A., Gautam, S., 2005. Hydrodynamic and water quality modeling of the A.R.M. Loxahatchee National Wildlife Refuge – Phase 1: preparation of data – data acquisition and processing. University of Louisiana at Lafayette, Lafayette, LA, 248 pp.

Miller, R., Meselhe, E.A., 2008. Louisiana Chenier Plain regional hydrodynamic and salinity numerical model, Proceedings of the Tenth International Conference on Estuarine and Coastal Modeling Congress 2007, 407-426.

Min, J.H., and Wise, W.R., 2009. Simulating short-circuiting flow in a constructed wetland: the implications of bathymetry and vegetation effects. Hydrol. Process. 23(6), 830–841.

Nepf, H.M., Mugnier, C.G., Zavistoski, R.A., 1997. The effects of vegetation on longitudinal dispersion. Estuarine, Coastal and Shelf Science 44 (6), 675.

Newman, S., Reddy, K.R., DeBusk, W.F., Wang, G.S., Fischer, M.M., 1997. Spatial distribution of soil nutrients in a northern Everglades marsh: Water Conservation Area 1. Soil Science Society of America 61 (4), 1275-1283.

Patro, S., Chatterjee, C., Mohanty, S., Singh, R., Raghuwanshi, N.S., 2009. Flood inundation modeling using MIKE FLOOD and remote sensing data, Journal of the Indian Society of Remote Sensing 37(1), 107-118.

Paudel, R., Min, J.-H., and Jawitz, J. W. (2010). "Management scenario evaluation for a large treatment wetland using a spatio-temporal phosphorus transport and cycling model." Ecological Engineering, 36(2010), 1627-1638.

Richardson, J.R., Bryant, W.L., Kitchens, W.M., Mattson, J.E., Pope, K.R., 1990. An evaluation of refuge habitats and relationships to water quality, quantity, and hydroperiod: A synthesis report. Florida Cooperative Fish and Wildlife Research Unit, University of Florida, Gainesville.

Roth, B.W., 2009. Modeling hydrodynamics and water quality in the Arthur R. Marshall Loxahatchee National Wildlife Refuge. Master thesis, University of Louisiana at Lafayette.

SFWMM, 2000. Florida Land Use and Cover Classification System (FLUCCS).

SFWMD, 2005a. Documentation of the South Florida Water Management Model Version 5.5. South Florida Water Management District, West Palm Beach, FL.

SFWMD, 2005b. Conceptual plan for preserving the soft water rainfall-based ecosystem of the A.R.M. Loxahatchee National Wildlife Refuge. South Florida Water Management District, West Palm Beach, FL.

Surratt, D.D., Waldon, M.G., Harwell, M.C., Aumen, N.G., 2008. Time-series and spatial tracking of polluted canal water intrusion into wetlands of a national wildlife refuge in Florida, USA. Wetlands 28 (1), 176-183.

Swift, D.R., 1981. Preliminary investigations of periphyton and water quality relationships in the Everglades Water Conservation Areas: February 1978 - August 1979. DRE-131, South Florida Water Management District, West Palm Beach, FL.

Swift, D.R., 1984. Periphyton and water quality relationships in the Everglades water conservation areas. Environments of South Florida Present and Past II. Gleasoned, P.J. (Ed.). Miami Geological Society, Coral Gables, FL, 97-117. < http://mwaldon.com/Loxahatchee/GrayLiterature/Swift-1984.PDF >.

Swift, D.R., Nicholas, R.B., 1987. Periphyton and water quality relationships in the Everglades Water Conservation Areas: 1978-1982. DRE-233, South Florida Water Management District, West Palm Beach, FL. < http://mwaldon.com/Loxahatchee/GrayLiterature/Swift-1987.pdf>.

Tsanis, I.K., Prescott, K.L., Shen, H., 1998. Modeling of phosphorus and suspended solids in Cootes Paradise marsh. Ecological Modeling 114, 1-17.

Thompson, J.R., Sørenson, H. Refstrup, Gavin, H., Refsgaard, A., 2004. Application of the coupled MIKE SHE/MIKE 11 modeling system to a lowland wet grassland in southeast England. Journal of Hydrology 293, 151–179.

USACE, 1994. Environmental assessment: modification of the Regulation Schedule Water Conservation Area No. 1. U.S. Army Corps of Engineers, Jacksonville, FL. <http://mwaldon.com/Loxahatchee/GrayLiterature/USACE-1995-Lox-Regulation-Schedule.pdf >.

USFWS, 2000. Arthur R. Marshall Loxahatchee National Wildlife Refuge Comprehensive Conservation Plan. U.S. Fish and Wildlife Service, Boynton Beach, Florida. <http://loxahatchee.fws.gov>.

USFWS, 2007. A.R.M. Loxahatchee National Wildlife Refuge - Enhanced Monitoring and Modeling Program - 2nd Annual Report. Report LOXA06-008. U.S. Fish and Wildlife Service, Boynton Beach, FL. <http://sofia.usgs.gov/lox_monitor_model/reports/>

Wang, H.Q., Meselhe, E.A., Waldon, M.G., Surratt, D., Abdou, S., Chen, C.F., Harwell, M.C., 2008. Compartment delineation for a wetland water quality model in the northern Everglades, Florida, USA. Journal of Environmental Hydrology 16, Paper 36.

Wang, H., Waldon, M.G., Meselhe, E.A., Arceneaux, J.C., Chen, C.F., Harwell, M.C., 2009. Surface water sulfate dynamics in the northern Florida Everglades, USA. Journal of Environmental Quality 38, 734-741.

Welter, D., 2002. Loxahatchee National Wildlife Refuge HSE model. South Florida Water Management District, West Palm Beach, FL.

Zhang, Y., Li, C., Trettin, C.C., Li, H., and Sun, G., 2002. An integrated model of soil, hydrology, and vegetation for carbon dynamics in wetland ecosystems. Global Biogeochem. Cycles 16(4), 1-17.